Projection methods for stochastic structural dynamics

S Adhikari

Zienkiewicz Centre for Computational Engineering, College of Engineering, Swansea University, Bay Campus, Swansea, Wales, UK, Email: S.Adhikari@swansea.ac.uk
Twitter: @ProfAdhikari, Web: http://engweb.swan.ac.uk/~adhikaris
S E Pryse and **A Kundu**

14th International Conference on Vibration Engineering and Technology Of Machinery (VETOMAC XIV), Lisbon, Portugal, in September 10 - 13, 2018.

ZCCE

Swansea University
Prifysgol Abertawe

Outline

Swansea University
Prifysgol Abertawe

Mathematical models for dynamic systems

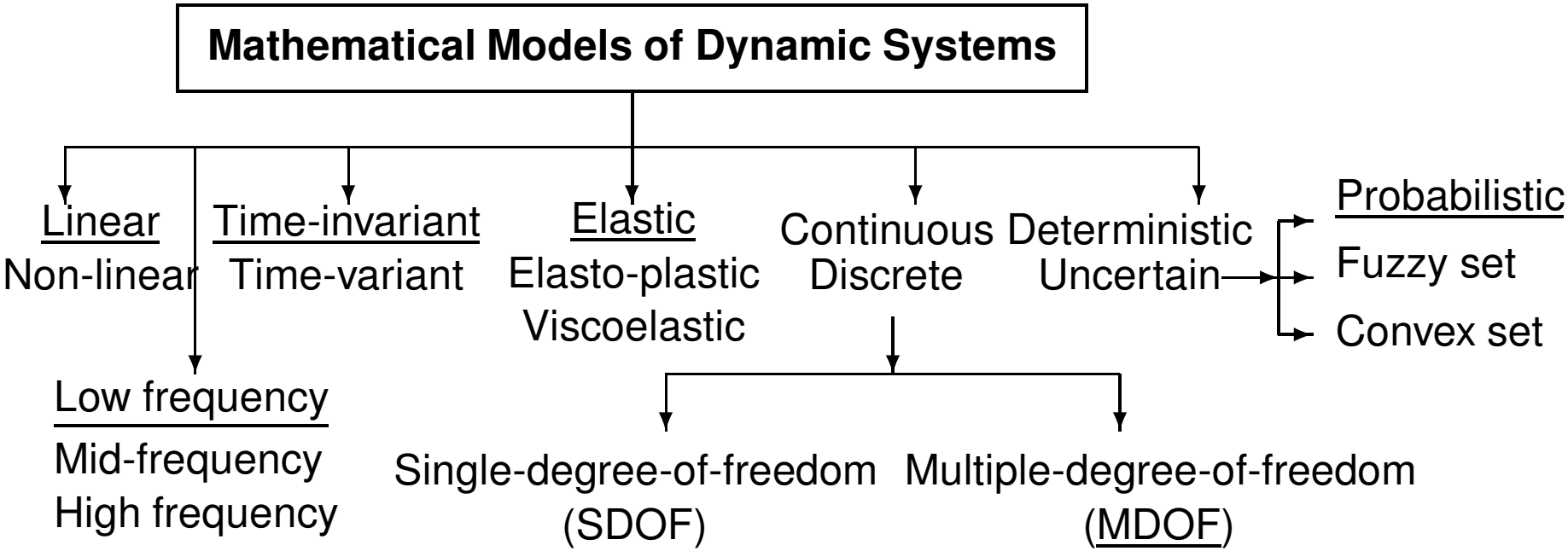

A general overview of computational mechanics

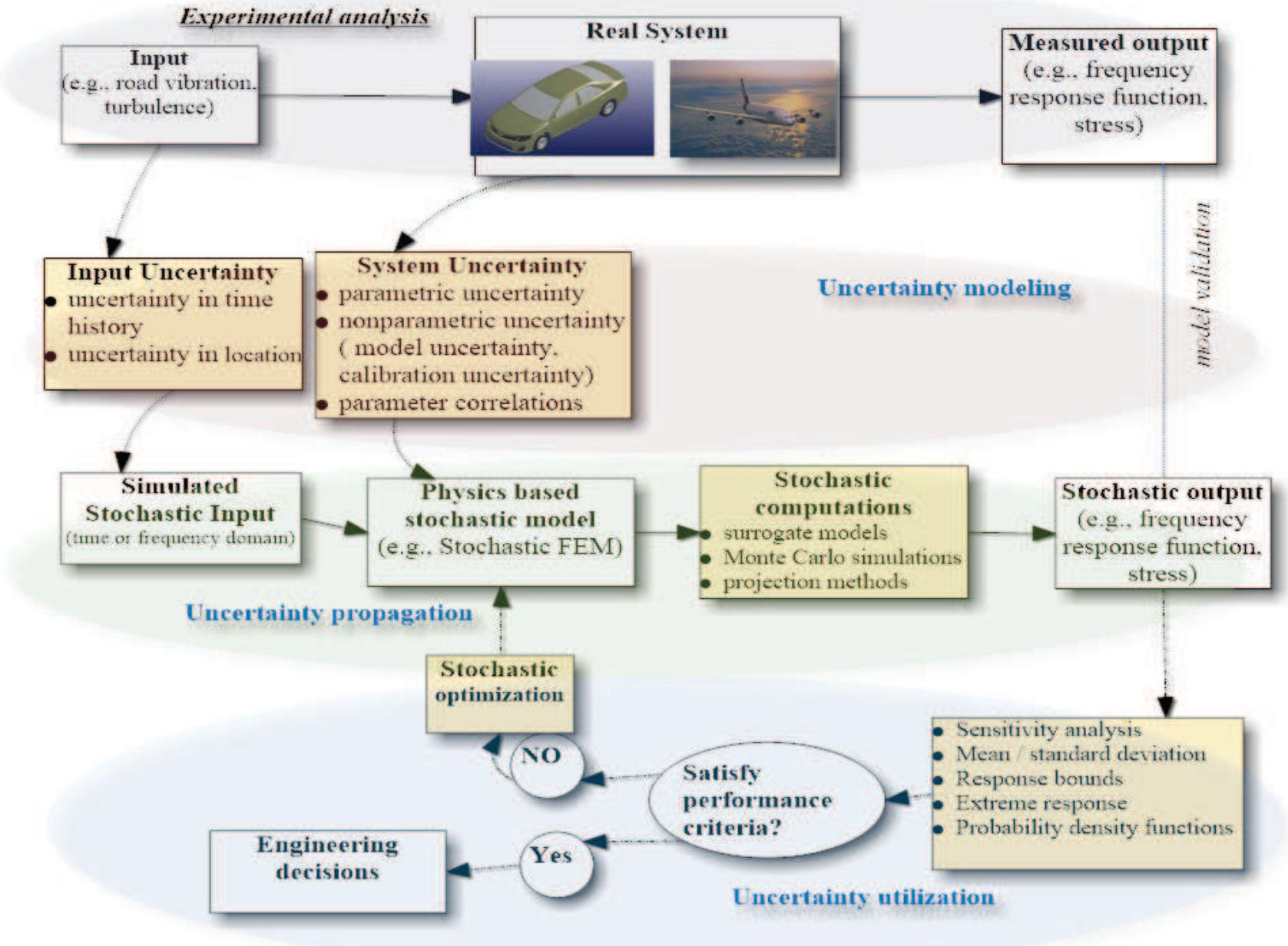

Uncertainty in structural dynamical systems

Many structural dynamic systems are manufactured in a production line (nominally identical systems). On the other hand, some models are complex! Complex models can have ‘errors’ and/or ‘lack of knowledge’ in its formulation.

Model quality

The quality of a model of a dynamic system depends on the following three factors:

- *Fidelity to (experimental) data:*
  The results obtained from a numerical or mathematical model undergoing a given excitation force should be close to the results obtained from the vibration testing of the same structure undergoing the same excitation.
- *Robustness with respect to (random) errors:*
  Errors in estimating the system parameters, boundary conditions and dynamic loads are unavoidable in practice. The output of the model should not be very sensitive to such errors.
- *Predictive capability:*
  In general it is not possible to experimentally validate a model over the entire domain of its scope of application. The model should predict the response well beyond its validation domain.

Sources of uncertainty

Different sources of uncertainties in the modeling and simulation of dynamic systems may be attributed, but not limited, to the following factors:

- Mathematical models: equations (linear, non-linear), geometry, damping model (viscous, non-viscous, fractional derivative), boundary conditions/initial conditions, input forces.
- Model parameters: Young's modulus, mass density, Poisson's ratio, damping model parameters (damping coefficient, relaxation modulus, fractional derivative order).
- Numerical algorithms: weak formulations, discretisation of displacement fields (in finite element method), discretisation of stochastic fields (in stochastic finite element method), approximate solution algorithms, truncation and roundoff errors, tolerances in the optimization and iterative methods, artificial intelligent (AI) method (choice of neural networks).
- Measurements: noise, resolution (number of sensors and actuators), experimental hardware, excitation method (nature of shakers and hammers), excitation and measurement point, data processing (amplification, number of data points, FFT), calibration.

Swansea University
Prifysgol Abertawe

Few general questions

- How does system uncertainty impact the dynamic response?
- How can we model uncertainty in dynamic systems? Do we ‘know’ the uncertainties?
- How can we efficiently quantify uncertainty in the dynamic response for large multi degrees of freedom systems?
- What about using ‘black box’ type response surface methods?
- Can we use modal analysis for stochastic systems? Does stochastic systems has natural frequencies and mode shapes as we understand them?
- What about the computational cost? Can we compute stochastic response ‘cheaply’? What are the consequences of cheap computational techniques?

Swansea University
Prifysgol Abertawe

Stochastic partial differential equation

We consider a stochastic partial differential equation (PDE) for a linear dynamic system

$$\rho(\mathbf{r},\theta)\frac{\partial^2 U(\mathbf{r},t,\theta)}{\partial t^2}+\mathcal{L}_\alpha\frac{\partial U(\mathbf{r},t,\theta)}{\partial t}+\mathcal{L}_\beta U(\mathbf{r},t,\theta)=p(\mathbf{r},t) \tag{1}$$

The stochastic operator $\mathcal{L}_\beta$ can be

- $\mathcal{L}_\beta \equiv \frac{\partial}{\partial x}AE(x,\theta)\frac{\partial}{\partial x}$ axial deformation of rods
- $\mathcal{L}_\beta \equiv \frac{\partial^2}{\partial x^2}EI(x,\theta)\frac{\partial^2}{\partial x^2}$ bending deformation of beams

$\mathcal{L}_\alpha$ denotes the stochastic damping, which is mostly proportional in nature.

Here $\alpha,\beta : \mathbb{R}^d \times \Theta \to \mathbb{R}$ are stationary square integrable random fields, which can be viewed as a set of random variables indexed by $\mathbf{r} \in \mathbb{R}^d$. Based on the physical problem the random field $a(\mathbf{r},\theta)$ can be used to model different physical quantities (e.g., $AE(x,\theta)$, $EI(x,\theta)$).

Discretisation of random fields

- The random process $a(\mathbf{r}, \theta)$ can be expressed in a generalized Fourier type of series known as the Karhunen-Loève expansion

$$a(\mathbf{r}, \theta) = a_0(\mathbf{r}) + \sum_{i=1}^{\infty} \sqrt{\nu_i} \xi_i(\theta) \varphi_i(\mathbf{r}) \tag{2}$$

- Here $a_0(\mathbf{r})$ is the mean function, $\xi_i(\theta)$ are uncorrelated standard Gaussian random variables, ν_i and $\varphi_i(\mathbf{r})$ are eigenvalues and eigenfunctions satisfying the integral equation

$$\int_{\mathcal{D}} C_a(\mathbf{r}_1, \mathbf{r}_2) \varphi_j(\mathbf{r}_1) \mathrm{d}\mathbf{r}_1 = \nu_j \varphi_j(\mathbf{r}_2), \quad \forall\, j = 1, 2, \cdots \tag{3}$$

Exponential autocorrelation function

- The autocorrelation function:

$$C(x_1, x_2) = e^{-|x_1 - x_2|/b} \tag{4}$$

- The underlying random process $H(x, \theta)$ can be expanded using the Karhunen-Loève (KL) expansion in the interval $-a \leq x \leq a$ as

$$H(x, \theta) = \sum_{j=1}^{\infty} \xi_j(\theta) \sqrt{\lambda_j} \varphi_j(x) \tag{5}$$

- Using the notation $c = 1/b$, the corresponding eigenvalues and eigenfunctions for odd j and even j are given by

$$\lambda_j = \frac{2c}{\omega_j^2 + c^2}, \qquad \varphi_j(x) = \frac{\cos(\omega_j x)}{\sqrt{a + \dfrac{\sin(2\omega_j a)}{2\omega_j}}}, \qquad \text{where} \quad \tan(\omega_j a) = \frac{c}{\omega_j}, \tag{6}$$

$$\lambda_j = \frac{2c}{\omega_j^2 + c^2}, \qquad \varphi_j(x) = \frac{\sin(\omega_j x)}{\sqrt{a - \dfrac{\sin(2\omega_j a)}{2\omega_j}}}, \qquad \text{where} \quad \tan(\omega_j a) = \frac{\omega_j}{-c} \tag{7}$$

KL expansion

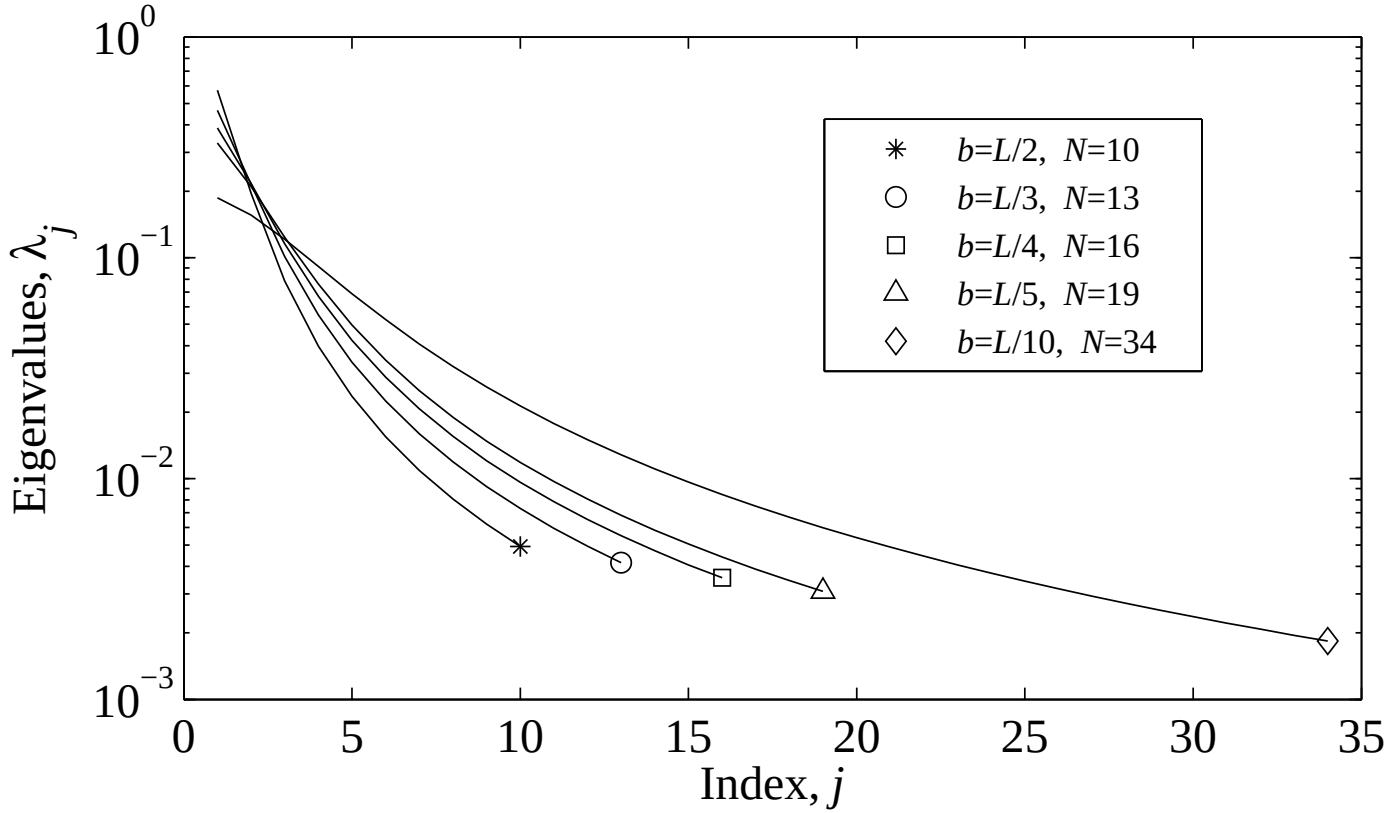

The eigenvalues of the Karhunen-Loève expansion for different correlation lengths, b, and the number of terms, N, required to capture 90% of the infinite series. An exponential correlation function with unit domain (i.e., $a = 1/2$) is assumed for the numerical calculations. The values of N are obtained such that $\lambda_N/\lambda_1 = 0.1$ for all correlation lengths. Only eigenvalues greater than λ_N are plotted.

Example: A beam with random properties

- The equation of motion of an undamped Euler-Bernoulli beam of length L with random bending stiffness and mass distribution:

$$\frac{\partial^2}{\partial x^2}\left[EI(x,\theta)\frac{\partial^2 Y(x,t)}{\partial x^2}\right] + \rho A(x,\theta)\frac{\partial^2 Y(x,t)}{\partial t^2} = p(x,t) \tag{8}$$

- $Y(x,t)$: transverse flexural displacement, $EI(x)$: flexural rigidity, $\rho A(x)$: mass per unit length, and $p(x,t)$: applied forcing. Consider

$$EI(x,\theta) = EI_0\left(1+\epsilon_1 F_1(x,\theta)\right) \tag{9}$$

$$\text{and} \quad \rho A(x,\theta) = \rho A_0\left(1+\epsilon_2 F_2(x,\theta)\right) \tag{10}$$

The subscript 0 indicates the mean values, $0 < \epsilon_i << 1$ (i=1,2) are deterministic constants and the random fields $F_i(x,\theta)$ are taken to have zero mean, unit standard deviation and covariance $R_{ij}(\xi)$.

Random beam element

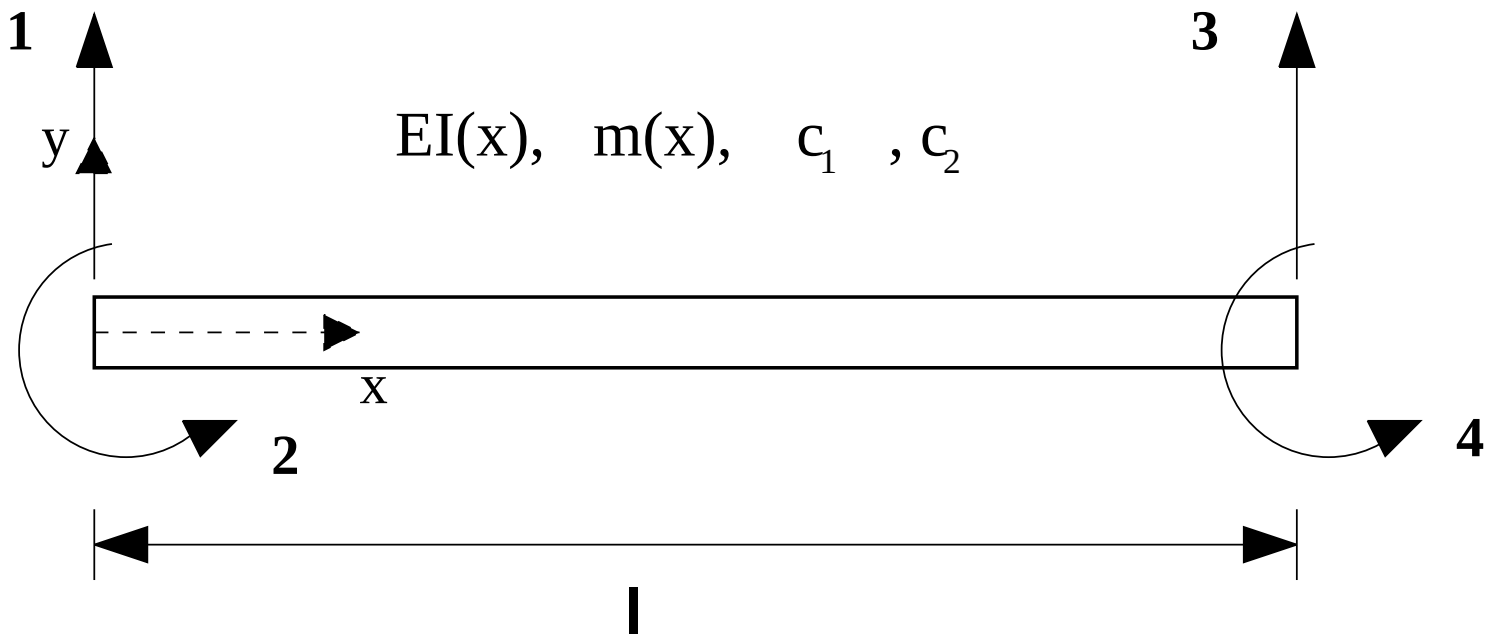

Random beam element in the local coordinate.

Realisations of the random field

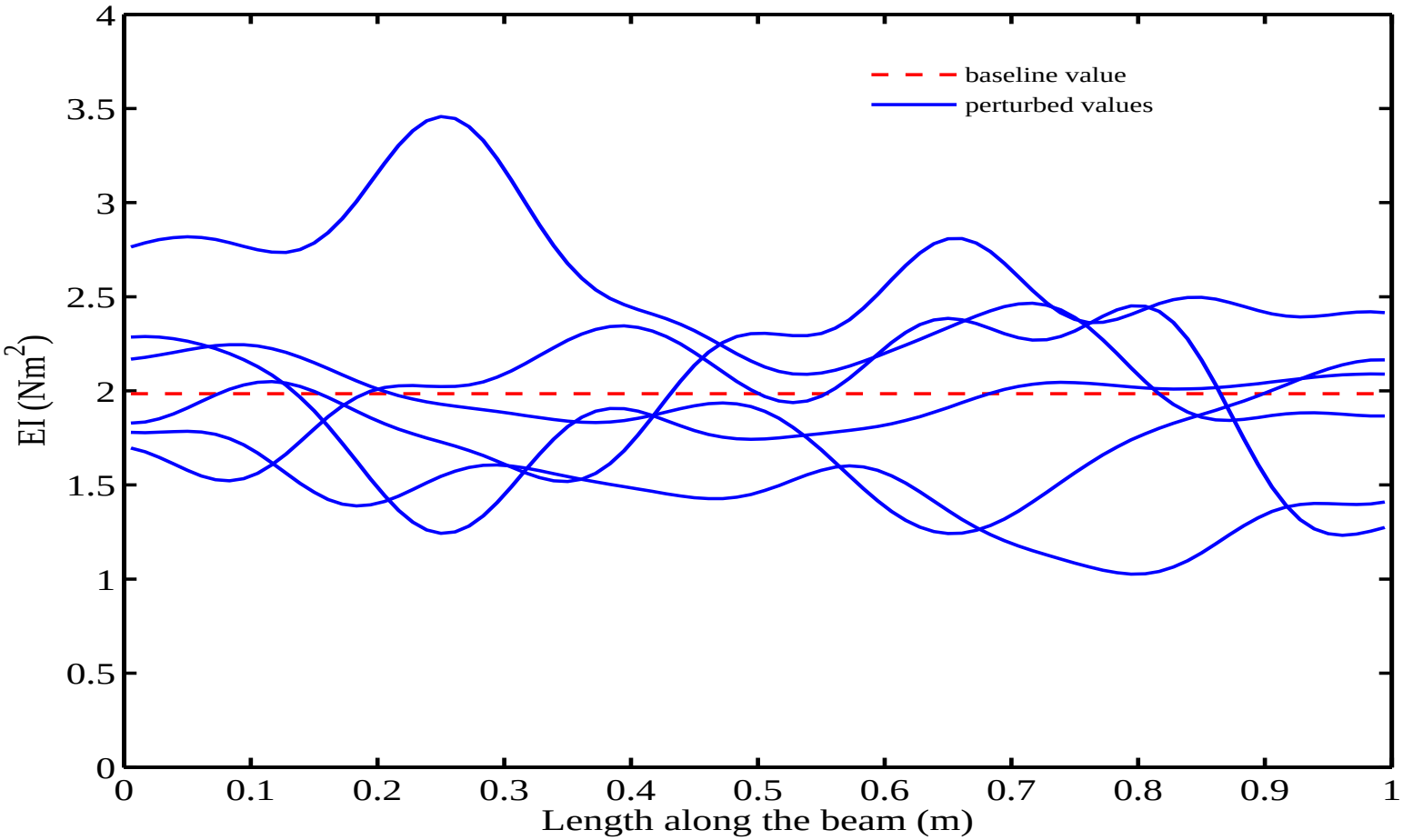

Some random realizations of the bending rigidity EI of the beam for correlation length $b = L/3$ and strength parameter $\epsilon_1 = 0.2$ (mean 2.0×10^5). Thirteen terms have been used in the KL expansion.

Example: A beam with random properties

- We express the shape functions for the finite element analysis of Euler-Bernoulli beams as

$$\mathbf{N}(x) = \mathbf{\Gamma}\,\mathbf{s}(x) \tag{11}$$

- where

$$\mathbf{\Gamma} = \begin{bmatrix} 1 & 0 & \frac{-3}{{\ell_e}^2} & \frac{2}{{\ell_e}^3} \\ 0 & 1 & \frac{-2}{{\ell_e}^2} & \frac{1}{{\ell_e}^2} \\ 0 & 0 & \frac{3}{{\ell_e}^2} & \frac{-2}{{\ell_e}^3} \\ 0 & 0 & \frac{-1}{{\ell_e}^2} & \frac{1}{{\ell_e}^2} \end{bmatrix} \quad \text{and} \quad \mathbf{s}(x) = \begin{bmatrix} 1, & x, & x^2, & x^3 \end{bmatrix}^T \tag{12}$$

- The element stiffness matrix:

$$\mathbf{K}_e(\theta) = \int_0^{\ell_e} \mathbf{N}''(x) EI(x,\theta) \mathbf{N}''^T(x) dx = \int_0^{\ell_e} EI_0 \left(1 + \epsilon_1 F_1(x,\theta)\right) \mathbf{N}''(x) \mathbf{N}''^T(x) \tag{13}$$

Example: A beam with random properties

- Expanding the random field $F_1(x,\theta)$ in KL expansion

$$\mathbf{K}_e(\theta) = \mathbf{K}_{e0} + \mathbf{\Delta K}_e(\theta) \tag{14}$$

- where the deterministic and random parts are

$$\mathbf{K}_{e0} = EI_0 \int_0^{\ell_e} \mathbf{N}^{''}(x)\mathbf{N}^{''T}(x)\,dx \quad \text{and} \quad \mathbf{\Delta K}_e(\theta) = \epsilon_1 \sum_{j=1}^{N_{\mathrm{K}}} \xi_{\mathrm{K}j}(\theta)\sqrt{\lambda_{\mathrm{K}j}}\mathbf{K}_{ej} \tag{15}$$

- The constant N_{K} is the number of terms retained in the Karhunen-Loève expansion and $\xi_{\mathrm{K}j}(\theta)$ are uncorrelated Gaussian random variables with zero mean and unit standard deviation. The constant matrices $\mathbf{K}_{ej}$ can be expressed as

$$\mathbf{K}_{ej} = EI_0 \int_0^{\ell_e} \varphi_{\mathrm{K}j}(x_e + x)\mathbf{N}^{''}(x)\mathbf{N}^{''T}(x)\,dx \tag{16}$$

Example: A beam with random properties

- The mass matrix can be obtained as

$$\mathbf{M}_e(\theta) = \mathbf{M}_{e_0} + \mathbf{\Delta M}_e(\theta) \tag{17}$$

- The deterministic and random parts is given by

$$\mathbf{M}_{e_0} = \rho A_0 \int_0^{\ell_e} \mathbf{N}(x)\mathbf{N}^T(x)\, dx \quad \text{and} \quad \mathbf{\Delta M}_e(\theta) = \epsilon_2 \sum_{j=1}^{N_{\mathrm{M}}} \xi_{\mathrm{M}j}(\theta)\sqrt{\lambda_{\mathrm{M}j}}\mathbf{M}_{ej} \tag{18}$$

- The constant N_{M} is the number of terms retained in Karhunen-Loève expansion and the constant matrices $\mathbf{M}_{ej}$ can be expressed as

$$\mathbf{M}_{ej} = \rho A_0 \int_0^{\ell_e} \varphi_{\mathrm{M}j}(x_e + x)\mathbf{N}(x)\mathbf{N}^T(x)\, dx \tag{19}$$

Both $\mathbf{K}_{ej}$ and $\mathbf{M}_{ej}$ can be obtained in closed-form.

Example: A beam with random properties

These element matrices can be assembled to form the global random stiffness and mass matrices of the form

$$\mathbf{K}(\theta) = \mathbf{K}_0 + \mathbf{\Delta K}(\theta) \quad \text{and} \quad \mathbf{M}(\theta) = \mathbf{M}_0 + \mathbf{\Delta M}(\theta). \tag{20}$$

Here the deterministic parts $\mathbf{K}_0$ and $\mathbf{M}_0$ are the usual global stiffness and mass matrices obtained form the conventional finite element method. The random parts can be expressed as

$$\mathbf{\Delta K}(\theta) = \epsilon_1 \sum_{j=1}^{N_{\mathrm{K}}} \xi_{\mathrm{K}j}(\theta)\sqrt{\lambda_{\mathrm{K}j}}\mathbf{K}_j \quad \text{and} \quad \mathbf{\Delta M}(\theta) = \epsilon_2 \sum_{j=1}^{N_{\mathrm{M}}} \xi_{\mathrm{M}j}(\theta)\sqrt{\lambda_{\mathrm{M}j}}\mathbf{M}_j \tag{21}$$

The element matrices $\mathbf{K}_{ej}$ and $\mathbf{M}_{ej}$ can be assembled into the global matrices $\mathbf{K}_j$ and $\mathbf{M}_j$. The total number of random variables depend on the number of terms used for the truncation of the infinite series. This in turn depends on the respective correlation lengths of the underlying random fields.

Stochastic equation of motion

- The equation for motion for stochastic linear multiple-degrees-of-freedom dynamic systems is given by

$$\mathbf{M}(\theta)\ddot{\mathbf{u}}(t) + \mathbf{C}_0\dot{\mathbf{u}}(t) + \mathbf{K}(\theta)\mathbf{u}(t) = \mathbf{f}_0(t) \tag{22}$$

  with the initial conditions set as

$$\mathbf{u}(0) = 0 \in \mathbb{R}^N \qquad \text{and} \qquad \dot{\mathbf{u}}(0) = 0 \in \mathbb{R}^N \tag{23}$$

- In Equation (22) $\mathbf{M}(\theta)$ and $\mathbf{K}(\theta)$ denote the random mass and stiffness matrices respectively. $\mathbf{C}_0$ and $\mathbf{f}_0(t)$ denote the deterministic damping matrix and the deterministic applied force whilst t represents the time.
- The displacement is represented by $\mathbf{u}(t)$ and $\dot{(\bullet)}$ represents the time-derivative
- The random mass and stiffness matrices can be expressed as follows

$$\mathbf{M}(\theta) = \mathbf{M}_0 + \sum_{j=1}^{p_1} \mu_j(\theta)\mathbf{M}_j \tag{24}$$

$$\mathbf{K}(\theta) = \mathbf{K}_0 + \sum_{j=1}^{p_2} \nu_j(\theta)\mathbf{K}_j \tag{25}$$

Stochastic equation of motion

- $\mathbf{M}_0$ corresponds to the deterministic mass matrix and $\mathbf{K}_0$ to the deterministic stiffness matrix. $\mathbf{M}_i$ and $\mathbf{K}_i$ are symmetric matrices which contribute towards the random components of $\mathbf{M}(\theta)$ and $\mathbf{K}(\theta)$.
- The random mass matrix has been modelled with p_1 random variables whilst the random stiffness matrix contains p_2 random variables.
- $\mu_i(\theta)$ represents the random variables associated with the random mass matrix, and $\nu_i(\theta)$ represents the random variables associated with the random stiffness matrix.
- $\boldsymbol{\zeta}$ denotes a diagonal matrix which contains modal damping factors, thus

$$\boldsymbol{\zeta} = \text{diag}[\zeta_1, \zeta_2, \ldots \zeta_N] \in \mathbb{R}^{N \times N} \tag{26}$$

- It it assumed that the all the diagonal entries are equal, therefore $\zeta_1 = \zeta_2 = \cdots = \zeta_N$. In order to satisfy this condition, the damping matrix $\mathbf{C}_0$ takes the following form

$$\mathbf{C}_0 = 2\boldsymbol{\zeta}\mathbf{M}_0\sqrt{\mathbf{M}_0^{-1}\mathbf{K}_0} \tag{27}$$

We have made the assumption that the deterministic damping matrix has been simultaneously diagonalized with the mass and stiffness matrices by utilising the deterministic undamped eigenmodes.

Stochastic equation of motion

- In order to compute the dynamic response in the frequency domain, taking the Fourier transform of Equation (22) results in

$$[-\omega^2\mathbf{M}(\theta) + \mathrm{i}\omega\mathbf{C}_0 + \mathbf{K}(\theta)]\tilde{\mathbf{u}}(\omega,\theta) = \tilde{\mathbf{f}}_0(\omega) \tag{28}$$

  Here $\tilde{\mathbf{u}}$ and $\tilde{\mathbf{f}}_0$ are the dynamic response and the forcing in the frequency domain.
- The random variables associated with both the random mass and the stiffness matrices can be grouped so that $\xi_j(\theta) = \mu_j(\theta)$ for $j = 1, 2, \ldots p_1$ and $\xi_{j+p_1}(\theta) = \nu_j(\theta)$ for $j = 1, 2, \ldots p_2$. In turn, Equation (28) can be re-written and expressed as

$$\left(\mathbf{D}_0(\omega) + \sum_{j=1}^{M} \xi_j(\theta)\mathbf{D}_j(\omega)\right)\tilde{\mathbf{u}}(\omega,\theta) = \tilde{\mathbf{f}}_0(\omega) \tag{29}$$

  where $\mathbf{D}_0(\omega) \in \mathbb{C}^{N\times N}$ represents the complex deterministic part of the system and $\mathbf{D}_j(\omega) \in \mathbb{R}^{N\times N}$ the random components.
- The total number of random variables, M, can be computed through summing p_1 and p_2.

- For the given configuration, the expressions for $\mathbf{D}_0$ and $\mathbf{D}_j$ are as follows

$$\mathbf{D}_0(\omega) = -\omega^2 \mathbf{M}_0 + \mathrm{i}\omega \mathbf{C}_0 + \mathbf{K}_0 \tag{30}$$

$$\begin{aligned} \mathbf{D}_j(\omega) &= -\omega^2 \mathbf{M}_j \qquad \text{for} \quad j = 1, 2, \ldots, p_1 \\ \mathbf{D}_j(\omega) &= \mathbf{K}_{j-p_1} \qquad \text{for} \quad j = p_1 + 1, p_1 + 2, \ldots, p_1 + p_2 \end{aligned} \tag{31}$$

- Therefore by combining the definitions of $\mathbf{D}_0(\omega)$ and $\mathbf{D}_j(\omega)$ with Equation (29), all the necessary components have been obtained in order to solve the discretized system of equations in the frequency domain.
- Next we discuss general methods to obtain the solution for $\theta \in \mathbf{\Theta}$ and for every frequency value $\omega \in \Omega$.

Possibilities of solution types

The frequency domain response vector of the stochastic system is governed by

$$\left[-\omega^2\mathbf{M}(\boldsymbol{\xi}(\theta)) + i\omega\mathbf{C}_0 + \mathbf{K}(\boldsymbol{\xi}(\theta))\right]\widetilde{\mathbf{u}}(\omega,\theta) = \widetilde{\mathbf{f}}_0(\omega) \tag{32}$$

There are **two** broad approaches to solve this equation:

- The direct Monte Carlo Simulation (MCS) which involves the generation of samples in the space θ for all frequency values ω.
- Reduced Order Methods (ROM), which generally involve a projection in a suitable space and minimising certain error norms. Some possibilities:

$$\begin{aligned}
\widetilde{\mathbf{u}}(\omega,\theta) &= \sum_{k=1}^{P_1} H_k(\boldsymbol{\xi}(\theta))\mathbf{u}_k(\omega) \\
\text{or} \quad &= \sum_{k=1}^{P_2} \Gamma_k(\omega,\boldsymbol{\xi}(\theta))\phi_k \\
\text{or} \quad &= \sum_{k=1}^{P_3} a_k(\omega)H_k(\boldsymbol{\xi}(\theta))\phi_k \\
\text{or} \quad &= \sum_{k=1}^{P_4} a_k(\omega)H_k(\boldsymbol{\xi}(\theta))\mathbf{U}_k(\boldsymbol{\xi}(\theta)) \quad \ldots \text{ etc.}
\end{aligned} \tag{33}$$

Computational paradigm for ROM

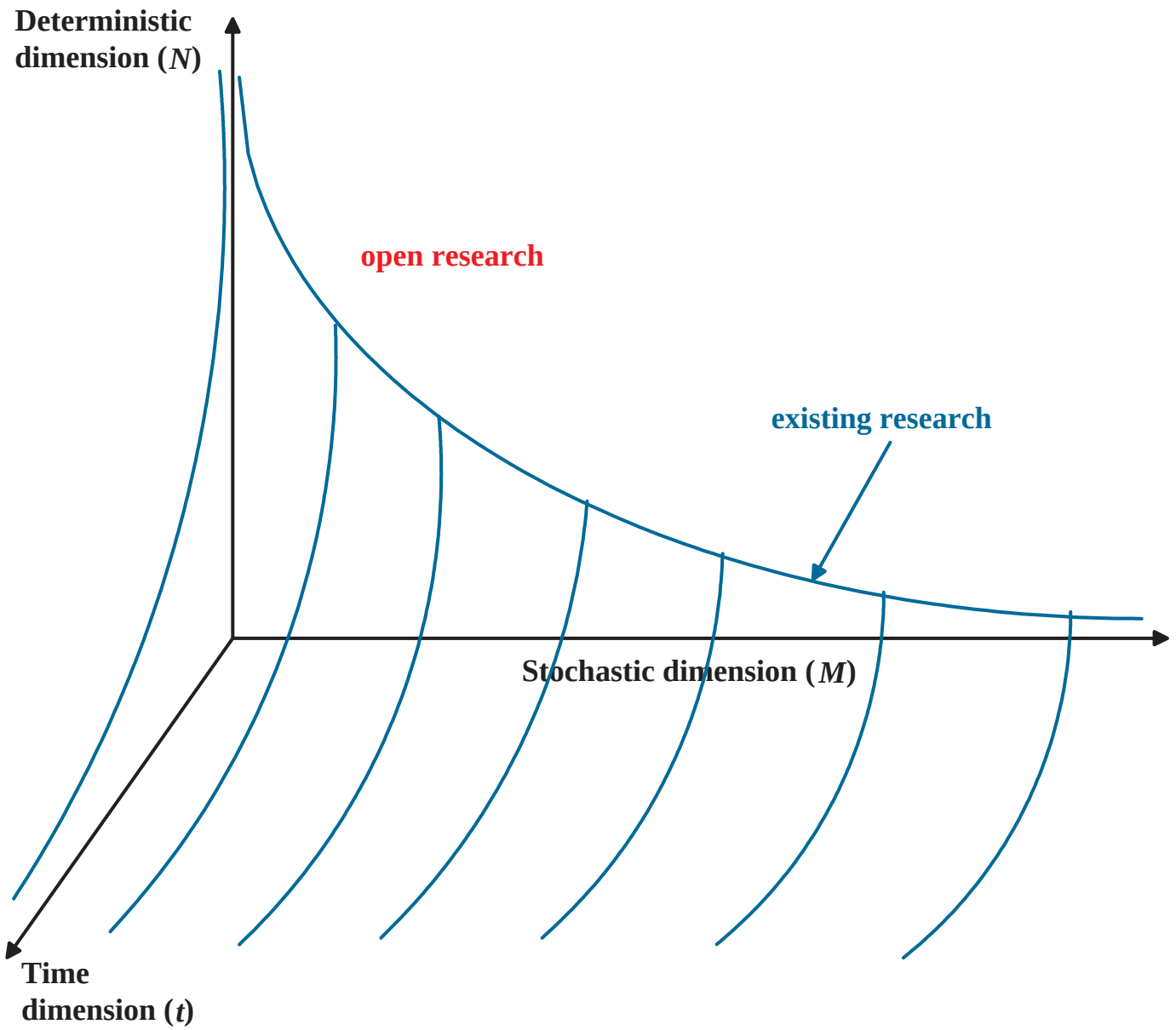

Polynomial Chaos expansion

Polynomial Chaos Expansion (PCE) is a projection in the space of orthogonal polynomials. The orthogonal polynomial basis is derived using the probability density function of the underlying random variable.
The PCE can be written as

$$\mathbf{u}(\theta) = \sum_{k=1}^{P} H_k(\boldsymbol{\xi}(\theta))\mathbf{u}_k \tag{34}$$

where $H_k(\boldsymbol{\xi}(\theta))$ are the polynomial chaoses. We need to solve a $nP \times nP$ linear equation to obtain all $\mathbf{u}_k \in \mathbb{R}^n$.

$$\begin{bmatrix} \mathbf{A}_{0,0} & \cdots & \mathbf{A}_{0,P-1} \\ \mathbf{A}_{1,0} & \cdots & \mathbf{A}_{1,P-1} \\ \vdots & \vdots & \vdots \\ \mathbf{A}_{P-1,0} & \cdots & \mathbf{A}_{P-1,P-1} \end{bmatrix} \begin{Bmatrix} \mathbf{u}_0 \\ \mathbf{u}_1 \\ \vdots \\ \mathbf{u}_{P-1} \end{Bmatrix} = \begin{Bmatrix} \mathbf{f}_0 \\ \mathbf{f}_1 \\ \vdots \\ \mathbf{f}_{P-1} \end{Bmatrix} \tag{35}$$

The number of terms P increases exponentially with M:

M	2	3	5	10	20	50	100
2nd order PC	5	9	20	65	230	1325	5150
3rd order PC	9	19	55	285	1770	23425	176850

Polynomial Chaos expansion for dynamics

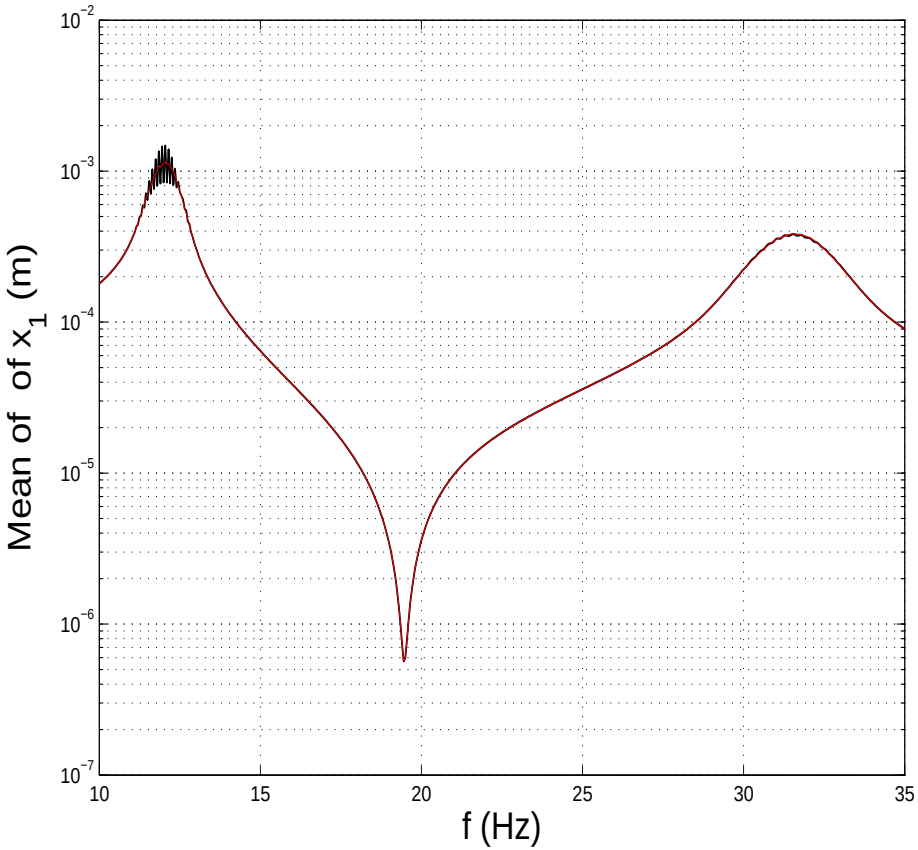

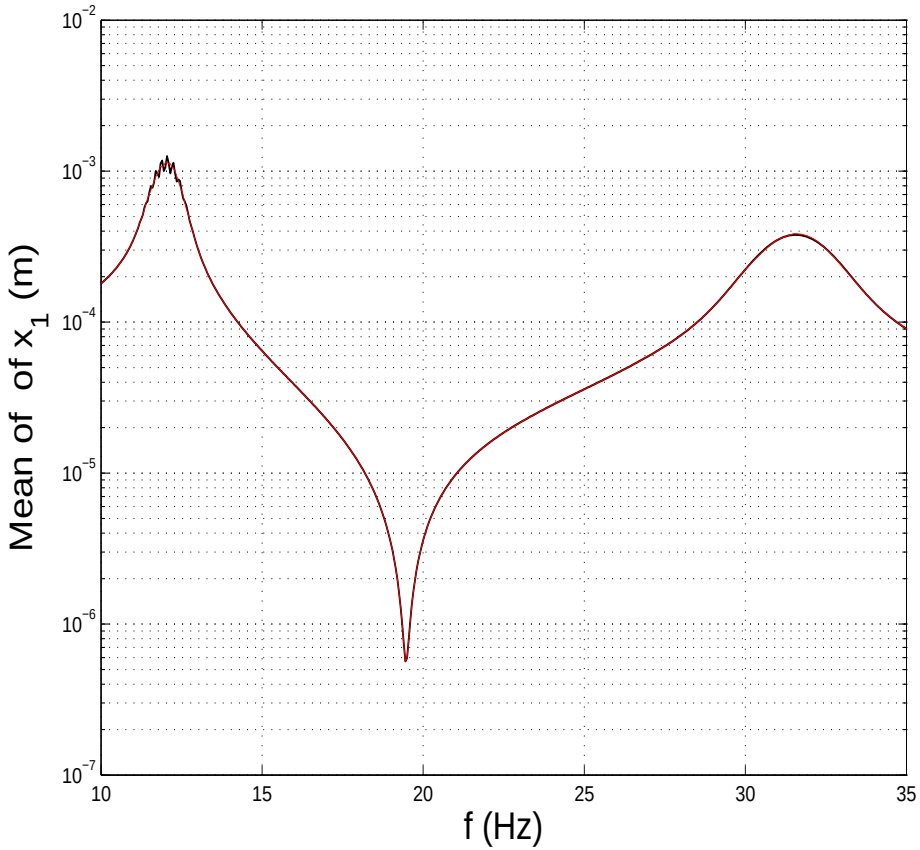

The application for classical PC directly leads to poor convergence of the frequency response around the resonance[1]

[1] Jacquelin, E., Adhikari, S., Sinou, J.-J., and Friswell, M. I., Polynomial chaos expansion and steady-state response of a class of random dynamical systems, ASCE Journal of Engineering Mechanics, Vol. 106, No. 6, 2015, pp. 061901:1-4.

Outline of the projection methods

- Three different projection methods are proposed. In order to compare the accuracy and effectiveness of the three proposed methods, the benchmark solution obtained by implementing a direct Monte Carlo approach [*DMCS*]

$$\tilde{\mathbf{u}}_{DMCS}(\omega,\theta) = [-\omega^2\mathbf{M}(\theta) + \mathrm{i}\omega\mathbf{C}_0 + \mathbf{K}(\theta)]^{-1}\tilde{\mathbf{f}}_0(\omega) \tag{36}$$

  for each frequency and realisation.
- We aim to propose a set of methods which computes the response by projecting onto a vector basis with scalar coefficients. The rationale behind proposing different methods is to analyse the effect of the nature of the coefficients and their associated vectors.

The first three methods have the following characteristics:

1. Projecting onto a stochastic basis with stochastic coefficients (M1)
2. Projecting onto a deterministic basis with stochastic coefficients (M2)
3. Projecting onto a deterministic basis with deterministic coefficients (M3)

The outline of the projection methods

- The basis vectors are kept independent of the frequency for computational efficiency.
- The response is represented by projecting onto a stochastic basis with stochastic coefficients

$$\tilde{\mathbf{u}}_1(\omega,\theta) = \sum_{j=1}^{N} \alpha_j(\omega,\theta)\mathbf{a}_j(\theta) \tag{37}$$

where $\alpha_j(\omega,\theta) \in \mathbb{C}$ denotes the random scalars which are contained in $\boldsymbol{\alpha}(\omega,\theta) \in \mathbb{C}^N$, and $\mathbf{a}_j(\theta) \in \mathbb{C}^N$ denotes the stochastic basis. These basis are contained within the matrix $\mathbf{a}(\theta) \in \mathbb{C}^{N\times N}$.

- The values of $\alpha_j(\omega,\theta)$ and $\mathbf{a}_j(\theta)$ can be obtained through numerous approaches.
- One such approach is by solving the following multi-objective optimisation problem:

$$\hat{\boldsymbol{\alpha}}(\omega,\theta) = \underset{\boldsymbol{\alpha}\in\mathbb{C}^N}{\arg\min} \; ||\tilde{\mathbf{u}}_{DMCS}(\omega,\theta) - \sum_{j=1}^{N} \alpha_j(\omega,\theta)1\hat{\mathbf{a}}_j(\theta)||_{L_2(\Theta)\times\mathbb{R}^N} \tag{38}$$

$$\hat{\mathbf{a}}(\theta) = \underset{\mathbf{a}\in\mathbb{C}^{N\times N}}{\arg\min} \; ||\tilde{\mathbf{u}}_{DMCS}(\omega,\theta) - \sum_{j=1}^{N} \hat{\alpha}_j(\theta)\mathbf{a}_j(\omega,\theta)||_{L_2(\Theta)\times\mathbb{R}^N} \tag{39}$$

The outline of the projection methods

- While the above approach gives the generic framework for the evaluation of the $\alpha(\omega, \theta)$ and $\mathbf{a}(\theta)$, the process can be computationally expensive due to the method's slow convergence rate.
- In order to avoid calculating $\tilde{\mathbf{u}}_{DMCS}(\omega, \theta)$, an expression for the above L_2 relative error can be obtained by observing the residual and by noting that the approximate error of the solution obtained when using Equation (37) is

$$\hat{\varepsilon}(\omega, \theta) = \tilde{\mathbf{u}}_1(\omega, \theta) - \tilde{\mathbf{u}}_{DMCS}(\omega, \theta) \tag{40}$$

- Here the error measure is defined by using the *DMCS* approach as a benchmark solution. A closed form of the error in the domain space of $\mathbf{D}(\omega, \theta)$ can be obtained. The residual can be re-written as

$$\mathbf{r}(\omega, \theta) = \mathbf{D}(\omega, \theta)\tilde{\mathbf{u}}_1(\omega, \theta) - \tilde{\mathbf{f}}_0(\omega) = \mathbf{D}(\omega, \theta)\left[\tilde{\mathbf{u}}_1(\omega, \theta) - \tilde{\mathbf{u}}^*(\omega, \theta)\right] \tag{41}$$

  where $\tilde{\mathbf{u}}^*(\omega, \theta)$ is the true solution of the system which can not be evaluated exactly.
- We can treat the solution of the *DMCS* approach, $\tilde{\mathbf{u}}_{DMCS}(\omega, \theta)$, as the benchmark solution.
- It is assumed the *DMCS* approach gives a better approximation of the true solution compared to $\tilde{\mathbf{u}}_1(\omega, \theta)$.

The outline of the projection methods

- Using $\mathbf{e}(\omega,\theta) = \tilde{\mathbf{u}}_1(\omega,\theta) - \tilde{\mathbf{u}}^*(\omega,\theta)$ as the true error, we write following Equation (41)

$$\mathbf{D}(\omega,\theta)\mathbf{e}(\omega,\theta) = \mathbf{r}(\omega,\theta) \tag{42}$$

- Thus the resulting true error vector is obtained as

$$\mathbf{e}(\omega,\theta) = \mathbf{D}^{-1}(\omega,\theta)\mathbf{r}(\omega,\theta) \tag{43}$$

- But $\mathbf{e}(\omega,\theta)$ can not be computed exactly and we have to resort to the approximate error indicator. We can define a bilinear form as $\bar{\mathbf{D}}(\mathbf{a},\mathbf{b}) = \langle \mathbf{D}(\omega,\theta)\mathbf{a}(\omega,\theta), \mathbf{b}(\omega,\theta)\rangle$ where $\langle\cdot,\cdot\rangle$ denotes an inner product in $L_2(\Theta)\times\mathbb{R}^N$.
- Hence, from Equation (43) we can deduce

$$\bar{\mathbf{D}}(\mathbf{e},\hat{\varepsilon}) = R_{\hat{\varepsilon}} \quad \text{where} \quad R_{\hat{\varepsilon}} = \langle \mathbf{r}(\omega,\theta), \hat{\varepsilon}(\omega,\theta)\rangle \tag{44}$$

- Using Cauchy-Schwarz inequality, we have

$$\left|\bar{\mathbf{D}}(\mathbf{e},\hat{\varepsilon})\right|^2 \leq \bar{\mathbf{D}}(\mathbf{e},\mathbf{e})\,\bar{\mathbf{D}}(\hat{\varepsilon},\hat{\varepsilon}) = ||\mathbf{e}||_E\,||\hat{\varepsilon}||_E \tag{45}$$

where $||\cdot||_E$ denotes the norm consistent with the bilinear form $\bar{\mathbf{D}}(\cdot,\cdot)$ on $L_2(\Theta)\times\mathbb{R}^N$ (analogous to the elastic potential energy norm for structural dynamic systems).

- Combining Equations (44) and (45) we obtain

$$\frac{|R_{\hat{\varepsilon}}|^2}{||\hat{\varepsilon}||_E} \leq ||\mathbf{e}||_E \tag{46}$$

  which indicates a lower bound for the true error $\mathbf{e}(\omega, \theta)$ in terms of the approximate error indicator $\hat{\varepsilon}(\omega, \theta)$.
- Note that the computation capacity required to implement such an approach is vastly higher than that required for the benchmark solution, a different approach is needed.

Projecting onto a stochastic basis with stochastic coefficients ($M1$)

- In order to implement a different approach, the generalised random eigenvalue problem for the undamped case is considered

$$\mathbf{K}(\theta)\phi_k(\theta) = \lambda_k(\theta)\mathbf{M}(\theta)\phi_k(\theta); \quad k = 1, 2, \ldots N \tag{47}$$

  where $\lambda_k(\theta)$ and $\phi_k(\theta)$ are the kth undamped random eigenvalue and eigenvector.
- For convenience, matrices that contain the whole set of random eigenvalues and eigenvectors are defined as follows

$$\begin{aligned} \mathbf{\Omega}^2(\theta) &= \mathrm{diag}\left[\lambda_1(\theta), \lambda_2(\theta), \ldots, \lambda_n(\theta)\right] \in \mathbb{R}^{N\times N} \quad \text{and} \\ \mathbf{\Phi}(\theta) &= \left[\phi_1(\theta), \phi_2(\theta), \ldots, \phi_n(\theta)\right] \in \mathbb{R}^{N\times N} \end{aligned} \tag{48}$$

- The eigenvalues are arranged in ascending order so $\lambda_1(\theta) < \lambda_2(\theta) < \ldots < \lambda_n(\theta)$ and their corresponding eigenvectors are mass normalised and arranged in the same order.
- It is apparent that

$$\begin{aligned} \mathbf{\Phi}^T(\theta)\mathbf{M}(\theta)\mathbf{\Phi}(\theta) &= \mathbf{I} \\ \mathbf{\Phi}^T(\theta)\mathbf{K}(\theta)\mathbf{\Phi}(\theta) &= \mathbf{\Omega}^2(\theta) \end{aligned} \tag{49}$$

Projecting onto a stochastic basis with stochastic coefficients ($M1$)

- As the undamped eigenvectors from a complete basis, it is possible to obtain the response of Equation (29) through projecting on the undamped eigenvectors.
- This can be done through using the previous identities and the dynamic equation

$$[-\omega^2\mathbf{M}(\theta) + \mathrm{i}\omega\mathbf{C}_0 + \mathbf{K}(\theta)]\tilde{\mathbf{u}}(\omega,\theta) = \tilde{\mathbf{f}}_0(\omega) \tag{50}$$

- The modal damping matrix is defined as follows

$$\mathbf{C}'(\theta) = \mathbf{\Phi}^T(\theta)\mathbf{C}_0\mathbf{\Phi}(\theta) = 2\zeta\mathbf{\Omega}(\theta) \tag{51}$$

where ζ corresponds to the diagonal modal damping matrix introduced in Equation (26).

- By using the following modal transformation $\tilde{\mathbf{u}}(\omega,\theta) = \mathbf{\Phi}(\theta)\bar{\mathbf{y}}(\omega,\theta)$ and by pre-multiplying Equation (50) with $\mathbf{\Phi}^T(\theta)$, we obtain

$$\mathbf{\Phi}^T(\theta)\left\{[-\omega^2\mathbf{M}(\theta) + \mathrm{i}\omega\mathbf{C}_0 + \mathbf{K}(\theta)]\mathbf{\Phi}(\theta)\right\}\bar{\mathbf{y}}(\omega,\theta) = \mathbf{\Phi}^T(\theta)\tilde{\mathbf{f}}_0(\omega) \tag{52}$$

Projecting onto a stochastic basis with stochastic coefficients ($M1$)

- By combining the modal damping matrix and the orthogonality relationships defined above, it can be shown that

$$\left[-\omega^2\mathbf{I} + 2\mathrm{i}\omega\boldsymbol{\zeta}\boldsymbol{\Omega}(\theta) + \boldsymbol{\Omega}^2(\theta)\right]\bar{\mathbf{y}}(\omega,\theta) = \boldsymbol{\Phi}^T(\theta)\tilde{\mathbf{f}}_0(\omega) \tag{53}$$

- Then by inverting $\left[-\omega^2\mathbf{I} + 2\mathrm{i}\omega\boldsymbol{\zeta}\boldsymbol{\Omega}(\theta) + \boldsymbol{\Omega}^2(\theta)\right]$, one has

$$\bar{\mathbf{y}}(\omega,\theta) = \left[-\omega^2\mathbf{I} + 2\mathrm{i}\omega\boldsymbol{\zeta}\boldsymbol{\Omega}(\theta) + \boldsymbol{\Omega}^2(\theta)\right]^{-1}\boldsymbol{\Phi}^T\tilde{\mathbf{f}}_0(\omega) \tag{54}$$

- As $\left[-\omega^2\mathbf{I} + 2\mathrm{i}\omega\boldsymbol{\zeta}\boldsymbol{\Omega}(\theta) + \boldsymbol{\Omega}^2(\theta)\right]$ is a diagonal matrix, its inverse is easy to compute and computationally inexpensive. By pre-multiplying both sides of the above equation with $\boldsymbol{\Phi}(\theta)$, we have

$$\boldsymbol{\Phi}(\theta)\bar{\mathbf{y}}(\omega,\theta) = \boldsymbol{\Phi}(\theta)\left[-\omega^2\mathbf{I} + 2\mathrm{i}\omega\boldsymbol{\zeta}\boldsymbol{\Omega}(\theta) + \boldsymbol{\Omega}^2(\theta)\right]^{-1}\boldsymbol{\Phi}^T(\theta)\tilde{\mathbf{f}}_0(\omega) \tag{55}$$

- By reintroducing $\tilde{\mathbf{u}}(\omega,\theta)$ for $\boldsymbol{\Phi}(\theta)\bar{\mathbf{y}}(\omega,\theta)$ a dynamic response in the frequency domain can be obtained

$$\tilde{\mathbf{u}}_1(\omega,\theta) = \boldsymbol{\Phi}(\theta)\left[-\omega^2\mathbf{I} + 2\mathrm{i}\omega\boldsymbol{\zeta}\boldsymbol{\Omega}(\theta) + \boldsymbol{\Omega}^2(\theta)\right]^{-1}\boldsymbol{\Phi}^T(\theta)\tilde{\mathbf{f}}_0(\omega) \tag{56}$$

- This expression can then be rewritten as a summation, where N corresponds to the number of degrees of freedom associated with the dynamic structure

$$\tilde{\mathbf{u}}_1(\omega,\theta) = \sum_{j=1}^{N} \alpha_j(\omega,\theta)\mathbf{a}_j(\theta) = \sum_{j=1}^{N} \left(\frac{\boldsymbol{\phi}_j^T(\theta)\tilde{\mathbf{f}}_0(\omega)}{\lambda_j(\theta) - \omega^2 + 2\mathrm{i}\sqrt{\lambda_j(\theta)}\omega\zeta} \right) \boldsymbol{\phi}_j(\theta) \tag{57}$$

- The response of the dynamic stochastic system under consideration has been represented in the same form as Equation (37).
- The random scalars, $\alpha_j(\omega,\theta)$, correspond to the expression $\frac{\boldsymbol{\phi}_j^T(\theta)\tilde{\mathbf{f}}_0}{\lambda_j(\theta)-\omega^2+2\mathrm{i}\sqrt{\lambda_j(\theta)}\omega\zeta}$.
- In turn, these random scalars are projected onto the space spanned by $\boldsymbol{\phi}_j(\theta)$.
- However, how to obtain the random eigenvalues and eigenvectors $\lambda_k(\theta)$ and $\boldsymbol{\phi}_k(\theta)$? [to be discussed]

Projecting onto a deterministic basis with stochastic coefficients (*M2*)

- If the value of N is large, the computational effort associated with computing the undamped random eigenvalues and eigenvectors can be considered very high.
- This is especially true if we sample for every $\theta \in \Theta$.
- In an attempt to lower the computational effort, we will consider a method that projects random scalars onto a deterministic basis

$$\tilde{\mathbf{u}}_2(\omega, \theta) = \sum_{j=1}^{N} \beta_j(\omega, \theta)\mathbf{b}_j \tag{58}$$

- The polynomial chaos approach is a method which projects onto a deterministic basis with stochastic coefficients

$$\tilde{\mathbf{u}}_2(\omega, \theta) = \sum_{k=1}^{P} H_k(\xi(\theta))\mathbf{u}_k(\omega) \tag{59}$$

where where $H_k(\xi(\theta))$ represents the polynomial chaoses (corresponding to the random scalars) and $\mathbf{u}_k$ represents unknown deterministic vectors that need to be determined.

Projecting onto a deterministic basis with stochastic coefficients (*M2*)

- The value of P is governed by the value of M and by the order of the polynomial chaos expansion. However the polynomial chaos approach is a notoriously costly method if the value of P or N is high. More importantly the basis $\mathbf{u}_k$ is a function of ω, thus this method does not comply with the desired form stated earlier in this section.
- Although mathematically strictly inconsistent, this method combines undamped random eigenvalues with undamped deterministic eigenvectors.
- By exchanging the undamped random eigenvectors seen in Equation (57) for their deterministic counterparts, the response vector for this new method can be expressed as

$$\tilde{\mathbf{u}}_2(\omega,\theta) = \sum_{j=1}^{N} \left(\frac{\phi_{0_j}^T \tilde{\mathbf{f}}_0}{\lambda_j(\theta) - \omega^2 + 2\mathrm{i}\sqrt{\lambda_j(\theta)}\omega\zeta} \right) \phi_{0_j} \tag{60}$$

  where ϕ_{0_j} denotes the jth deterministic undamped eigenvector.
- Therefore we aim to see if the vast majority of the stochastic nature of the system can be incorporated by only using the undamped random eigenvalues.

Projecting onto a deterministic basis with deterministic coefficients (*M*3)

- As a simplest scenario we consider the case of when all the eigensolutions are deemed deterministic. For this case, the response vector takes the following form

$$\tilde{\mathbf{u}}_3(\omega,\theta) = \sum_{j=1}^{N} \gamma_{0_j}(\omega)\mathbf{c}_j \tag{61}$$

  where $\gamma_{0_j}(\omega) \in \mathbb{C}$ and $\mathbf{c}_j \in \mathbb{C}^N$ are deterministic scalars and basis respectively.
- If both the undamped random eigenvalues and eigenvectors seen in Equation (57) are exchanged for their deterministic counterpart, the response vector can be expressed as

$$\tilde{\mathbf{u}}_3(\omega) = \sum_{j=1}^{N} \left(\frac{\boldsymbol{\phi}_{0_j}^T \tilde{\mathbf{f}}_0}{\lambda_{0_j} - \omega^2 + 2\mathrm{i}\sqrt{\lambda_{0_j}}\omega\zeta} \right) \boldsymbol{\phi}_{0_j} \tag{62}$$

  where λ_{0_j} and $\boldsymbol{\phi}_{0_j}$ denote the jth undamped deterministic eigenvalue and eigenvector respectively.
- Due to all the terms in Equation (62) being deterministic, the stochastic nature of the system is not at all incorporated into the response vector.

Projecting onto a deterministic basis with deterministic coefficients (*M*3)

- Equation (62) provides the deterministic solution and therefore can be established as a worst case scenario. However if the coefficient of variation associated with the stochastic process is low, this method expected to provide an adequate approximation of the mean of the true solution.
- If the matrices $\mathbf{U}_{DMCS} \in \mathbb{C}^{N\times m}$ and $\mathbf{U}_3 \in \mathbb{C}^{N\times m}$ contain the solution vectors for all realisations of a given frequency for the benchmark and *M*3 methods, the Frobenius norm of the relative error is given by

$$||\mathbf{U}_{DMCS} - \mathbf{U}_3||_F = \sqrt{\sum_{i=1}^{N}\sum_{j=1}^{m}\left|\{\mathbf{U}_{DMCS} - \mathbf{U}_3\}_{ij}\right|^2} \tag{63}$$

  where m corresponds to the number of realisations.
- If the matrices $\mathbf{U}_1 \in \mathbb{C}^{N\times m}$ and $\mathbf{U}_2 \in \mathbb{C}^{N\times m}$ are similarly defined for the *M*1 and *M*2 methods the following propositions can be made

$$||\mathbf{U}_{DMCS} - \mathbf{U}_1||_F \leq ||\mathbf{U}_{DMCS} - \mathbf{U}_2||_F \leq ||\mathbf{U}_{DMCS} - \mathbf{U}_3||_F \tag{64}$$

Critical review of the proposed methods

- Due to both the eigenvalues and the eigenvectors retaining their stochastic properties in $M1$ method, it is intuitively expected that the $M1$ method would induce the least amount of error.
- As the entire stochasticity of the response vector is expected to be captured by the stochastic eigenvalues in the $M2$ method, this method is not expected to outperform the $M1$ method. In a similar manner, as the $M3$ is deemed to be a worst-case scenario, naturally this method will not outperform both the $M1$ and $M2$ methods.
- At present, the computational time associated with both the $M1$ and $M2$ methods can be considered quite high, especially for a high degree of freedom finite element system.
- This is due to two reasons. The first being the large number of terms in the summations seen in Equations (57) and (60). At present, the number of terms in the series corresponds to the number of degrees of freedom. Secondly, calculating the random eiegnsolutions is computationally expensive.
- Combining these reasons with the need to simulate the methods for each $\theta \in \Theta$ accumulates to a high computational effort.

Approximating the undamped eigensolutions

- Calculating the exact undamped random eigensolutions can be extremely expensive, especially if the number of degrees of freedom is large.
- Thus a sensitivity approach to approximate the eigensolutions could computationally be a better option.
- The random eigenvalues can be approximated as

$$\lambda_j \approx \lambda_{j_0} + \sum_{k=1}^{M} \left(\frac{\partial \lambda_j}{\partial \xi_k} \right) \mathrm{d}\xi_k(\theta) \tag{65}$$

where λ_{j_0} is the jth deterministic undamped eigenvalue and $\mathrm{d}\xi_k(\theta)$ a set of Gaussian random variables with mean zero and unit variance.

- The derivative of the undamped random eigenvalues with respect to ξ_k can be obtained through differentiating and manipulating the eigenvalue equation and is expressed through this closed-form expression

$$\frac{\partial \lambda_j}{\partial \xi_k} = \frac{\phi_{0_j}^T \left[\frac{\partial \mathbf{K}}{\partial \xi_k} - \lambda_{0_j} \frac{\partial \mathbf{M}}{\partial \xi_k} \right] \phi_{0_j}}{\phi_{0_j}^T \mathbf{M}_0 \phi_{0_j}} \tag{66}$$

where λ_{0_j} and ϕ_{0_j} correspond to the deterministic undamped eigenvalues and eigenvectors.

Approximating the undamped eigensolutions

- As the deterministic undamped eigenvectors are mass normalised, the denominator in the above equation equates to one i.e. $\phi_{0_j}^T \mathbf{M}_0 \phi_{0_j} = 1$, thus resulting in

$$\frac{\partial \lambda_{0_j}}{\partial \xi_k} = \phi_{0_j}^T \left[\frac{\partial \mathbf{K}}{\partial \xi_k} - \lambda_{0_j} \frac{\partial \mathbf{M}}{\partial \xi_k} \right] \phi_{0_j} \tag{67}$$

- The values of both $\frac{\partial \mathbf{M}}{\partial \xi_k}$ and $\frac{\partial \mathbf{K}}{\partial \xi_k}$ are as follows

$$\begin{aligned} \frac{\partial \mathbf{M}}{\partial \xi_k} &= \begin{cases} \mathbf{M}_k, & \text{for } j = 1, 2, \ldots, p_1 \\ 0, & \text{otherwise} \end{cases} \\ \frac{\partial \mathbf{K}}{\partial \xi_k} &= \begin{cases} \mathbf{K}_{k-p_1}, & \text{for } k = p_1 + 1, p_1 + 2, \ldots, p_1 + p_2 \\ 0, & \text{otherwise} \end{cases} \end{aligned} \tag{68}$$

where $\mathbf{M}_k$ and $\mathbf{K}_k - p_1$ correspond to the random components of $\mathbf{M}(\theta)$ and $\mathbf{K}(\theta)$ introduced through Equations (24) and (25).

Approximating the undamped eigensolutions

- In a similar manner, the random undamped eigenvectors can also be expressed as

$$\phi_j \approx \phi_{j_0} + \sum_{k=1}^{M} \left(\frac{\partial \phi_j}{\partial \xi_k} \right) \mathrm{d}\xi_k(\theta) \tag{69}$$

  where ϕ_{j_0} is the jth deterministic undamped eigenvector.
- The derivative of the jth undamped random eigenvector with respect to ξ_k is expressed as a linear combination of deterministic eigenvectors

$$\frac{\partial \phi_j}{\partial \xi_k} = \sum_{r=1}^{N} \alpha_{jr} \phi_{0_r} \tag{70}$$

- The closed-form expression for $\frac{\partial \phi_j}{\partial \xi_k}$ is given by

$$\frac{\partial \phi_j}{\partial \xi_k} = -\frac{1}{2} \left(\phi_{j_0}^T \frac{\partial \mathbf{M}}{\partial \xi_k} \phi_{j_0} \right) + \sum_{i=1 \neq j}^{N} \frac{\phi_{k_0}^T \left[\frac{\partial \mathbf{K}}{\partial \xi_k} - \lambda_{j_0} \frac{\partial \mathbf{M}}{\partial \xi_k} \right] \phi_{j_0}}{\lambda_{j_0} - \lambda_{k_0}} \phi_{k_0} \tag{71}$$

- From the ordering of the eigenvalues it can be deduced that

$$\lambda_1 < \lambda_2 < \ldots < \lambda_N \tag{72}$$

  where λ_j corresponds to the jth eigenvalue.
- Recall that for scalar α_j the eigenvalues appear in the denominator

$$\alpha_j(\omega, \theta) = \frac{\boldsymbol{\phi}_j^T(\theta)\tilde{\mathbf{f}}_0}{\lambda_j(\theta) - \omega^2 + 2\mathrm{i}\sqrt{\lambda_j(\theta)}\omega\zeta} \tag{73}$$

- For the values of j satisfying $\lambda_j(\theta) + 2\mathrm{i}\sqrt{\lambda_j(\theta)}\omega\zeta > \omega^2$, it is apparent that the value of the denominator increases as the value of j increases.
- We use this observation to truncate the three series epressions proposed before.

Model order reduction using a reduced basis

- The reduced-order expressions are given by

$$\tilde{\mathbf{u}}_1(\omega,\theta) \approx \sum_{j=1}^{n_r} \left(\frac{\phi_j^T(\theta)\tilde{\mathbf{f}}_0}{\lambda_j(\theta) - \omega^2 + 2\mathrm{i}\sqrt{\lambda_j(\theta)}\omega\zeta} \right) \phi_j(\theta) \tag{74}$$

$$\tilde{\mathbf{u}}_2(\omega,\theta) \approx \sum_{j=1}^{n_r} \left(\frac{\phi_{0_j}^T\tilde{\mathbf{f}}_0}{\lambda_j(\theta) - \omega^2 + 2\mathrm{i}\sqrt{\lambda_j(\theta)}\omega\zeta} \right) \phi_{0_j} \tag{75}$$

$$\tilde{\mathbf{u}}_3(\omega) \approx \sum_{j=1}^{n_r} \left(\frac{\phi_{0_j}^T\tilde{\mathbf{f}}_0}{\lambda_{0_j} - \omega^2 + 2\mathrm{i}\sqrt{\lambda_{0_j}}\omega\zeta} \right) \phi_{0_j} \tag{76}$$

- Here $n_r < N \ll NP$. The value of n_r can be defined in two ways (a) the value can be predefined depending on the system under consideration (b) by selecting a value for ϵ which is sufficiently small, n_r can be selected such that $\lambda_{0_{(n_r)}}$ is the largest deterministic eigenvalue that satisfies $\frac{\lambda_{0_1}}{\lambda_{0_{(n_r)}}} > \epsilon$.
- If the accuracy of the truncated series is not sufficient, the accuracy can be improved by increasing the predefined value of n_r or selecting a lower value for ϵ.

Galerkin error minimisation

- Three different projection methods have been proposed.
- The first projects random scalars onto a stochastic basis whilst the second projects random scalars onto a deterministic basis. The third method projects deterministic scalars onto a deterministic basis.
- We have shown that it's possible to approximate the random eigensolutions that arise in the proposed methods in order to lower the computational effort.
- However, these approximations, in addition to the modal reduction, introduces error into the calculation.
- This has motivated an error minimisation technique through applying a Galerkin approach.
- As a result, the following three new projection methods are proposed:
  - Galerkin approach with projecting onto a stochastic basis with stochastic coefficients ($M1G$)
  - Galerkin approach with projecting onto a stochastic basis with deterministic coefficients ($M2G$)
  - Galerkin approach with projecting onto a deterministic basis with deterministic coefficients ($M3G$)

Swansea University
Prifysgol Abertawe

Galerkin+projecting onto a stochastic basis with stochastic coefficients (*M*1*G*)

- The response vector for the given case is modified to take the following series representation

$$\begin{aligned}\tilde{\mathbf{u}}_{1G}(\omega,\theta) &\approx \sum_{j=1}^{n_r} c_j(\omega,\theta)\left(\frac{\phi_j^T(\theta)\tilde{\mathbf{f}}_0}{\lambda_j(\theta)-\omega^2+2\mathrm{i}\sqrt{\lambda_j(\theta)}\omega\zeta}\right)\phi_j(\theta) \\ &= \sum_{j=1}^{n_r} c_j(\omega,\theta)\,\alpha_j(\omega,\theta)\,\phi_j(\theta)\end{aligned} \tag{77}$$

- Here $\alpha_j(\omega,\theta)$ and $\phi_j(\theta)$ correspond to the random scalars and random eigenvectors seen in Equation (57) whilst $c_j(\omega,\theta) \in \mathbb{C}$ are constants which need to be obtained for each realisation.
- This can be done by applying a sample based Galerkin approach. We initially consider the following residual

$$\mathbf{r}(\omega,\theta) = \left(\sum_{i=0}^{M}\mathbf{D}_i(\omega)\xi_i(\theta)\right)\left(\sum_{j=1}^{n_r} c_j(\omega,\theta)\alpha_j(\omega,\theta)\phi_j(\theta)\right) - \tilde{\mathbf{f}}_0(\omega) \in \mathbb{C}^N \tag{78}$$

where $\xi_0 = 1$ is used in order to simplify the summation.

Galerkin+projecting onto a stochastic basis with stochastic coefficients (*M*1*G*)

- By making the residual orthogonal to a basis function, the unknown $c_j(\omega,\theta)$ can be computed.
- As Equation (77) can be viewed as a projection onto a stochastic basis, the residual is made orthogonal to the undamped random eigenvectors

$$\mathbf{r}(\omega,\theta) \perp \phi_k(\theta) \qquad \forall \quad k = 1,2,\ldots n_r \tag{79}$$

- As a sample based Galerkin approach is considered, applying the orthogonality condition results in

$$\phi_k^T(\theta)\left[\left(\sum_{i=0}^{M}\mathbf{D}_i(\omega)\xi_i(\theta)\right)\left(\sum_{j=1}^{n_r}c_j(\omega,\theta)\alpha_j(\omega,\theta)\phi_j(\theta)\right) - \phi_k^T(\theta)\tilde{\mathbf{f}}_0(\omega)\right] = 0 \tag{80}$$

- Through manipulating Equation (80) it is possible to re-write the equation in the following form

$$\sum_{j=1}^{n_r}\underbrace{\left(\sum_{i=0}^{M}\left[\phi_k^T(\theta)\mathbf{D}_i(\omega)\phi_j(\theta)\right]\left[\xi_i(\theta)\alpha_j(\omega,\theta)\right]\right)}_{\mathbf{Z}_1(\omega,\theta)}\underbrace{c_j(\omega,\theta)}_{\mathbf{c}_1(\omega,\theta)} = \underbrace{\phi_k^T(\theta)\tilde{\mathbf{f}}_0(\omega)}_{\mathbf{y}_1(\omega)} \tag{81}$$

Galerkin+projecting onto a stochastic basis with stochastic coefficients (*M*1*G*)

- By defining the vector $\mathbf{c}_1(\omega,\theta) = [c_1(\omega,\theta)\, c_2(\omega,\theta) \ldots c_{n_r}(\omega,\theta)]^T$, Equation (81) can be re-written as

$$\mathbf{Z}_1(\omega,\theta)\mathbf{c}_1(\omega,\theta) = \mathbf{y}_1(\omega,\theta) \qquad j,k = 1,2,\ldots,n_r \tag{82}$$

- Here $\mathbf{Z}_{1_{kj}}(\omega,\theta) = \sum_{i=0}^{M} \left[\phi_k^T(\theta)\mathbf{D}_i(\omega)\phi_j(\theta)\right] \left[\xi_i(\theta)\alpha_j(\omega,\theta)\right]$; $\forall j,k = 1,2,\ldots n_r$ and $\mathbf{y}_1(\omega,\theta) = \phi_k^T(\theta)\tilde{\mathbf{f}}_0(\omega)$.
- The number of equations that need to be solved in order to calculate the unknown vector $\mathbf{c}(\omega,\theta)$ corresponds to the value of n_r.
- By increasing the number of terms from n_r to $n_r + 1$, the number of terms in $\mathbf{Z}_1(\omega,\theta)$ increases by $2n+1$.
- Therefore the lower the dimension of the reduced system, the fewer the number of equations that need to be solved. This is of importance as the given procedure needs to be repeated for every realisation and for every frequency under consideration.

Galerkin+projecting onto a stochastic basis with deterministic coefficients (*M2G*)

- The response contains undamped random eigenvalues and deterministic eigenvectors. The response vector with the Galerkin approach takes the following form

$$\begin{aligned}\tilde{\mathbf{u}}_{2G}(\omega,\theta) &\approx \sum_{j=1}^{n_r} c_j(\omega,\theta)\left(\frac{\boldsymbol{\phi}_{0_j}^T\tilde{\mathbf{f}}_0}{\lambda_j(\theta)-\omega^2+2\mathrm{i}\sqrt{\lambda_j(\theta)}\omega\zeta}\right)\boldsymbol{\phi}_{0_j} \\ &= \sum_{j=1}^{n_r} c_j(\omega,\theta)\,\beta_j(\omega,\theta)\,\boldsymbol{\phi}_{0_j}\end{aligned} \tag{83}$$

- Here $\beta_j(\omega,\theta)$ corresponds to the scalars introduced in Equation (60) and $\boldsymbol{\phi}_{0_j}$ to the deterministic eigenvectors also introduced in Equation (60).
- $c_j(\omega,\theta) \in \mathbb{C}$ are the unknown constants that need to obtained for each realisation of each frequency.
- The residual is projected onto deterministic eigenvectors rather than the random eigenvectors seen before.

Galerkin+projecting onto a stochastic basis with deterministic coefficients (*M2G*)

- The unknown constants $c_j(\omega,\theta)$ can be computed by solving the following set of linear equations.

$$\mathbf{Z}_2(\omega,\theta)\mathbf{c}_2(\omega,\theta) = \mathbf{y}_2(\omega) \qquad j,k = 1,2,\ldots,n_r \tag{84}$$

where $\mathbf{Z}_{2_{kj}}(\omega,\theta) = \sum_{i=0}^{M} \left[\phi_{0_k}^T \mathbf{D}_i(\omega)\phi_{0_j}\right]\left[\xi_i(\theta)\beta_j(\omega,\theta)\right]$;

$$\beta_j(\omega,\theta) = \sum_{j=1}^{n_r}\left(\frac{\phi_{0_j}^T\tilde{\mathbf{f}}_0}{\lambda_j(\theta)-\omega^2+2\mathrm{i}\sqrt{\lambda_j(\theta)}\omega\zeta}\right)$$

$$\mathbf{y}_2(\omega) = \phi_k^T(\theta)\tilde{\mathbf{f}}_0(\omega) \quad \forall \quad j,k = 1,2,\ldots n_r$$

and $\mathbf{c}_2(\omega,\theta)$ is a vector that contains the unknown constants $c_j(\omega,\theta)$

- The number of equations that need to be solved to compute the unknown coefficients corresponds to the number of modes retained in the reduced model.
- Note that this procedure needs to be repeated for every realisation and for every $\omega \in \Omega$.

Galerkin+projecting onto a deterministic basis with deterministic coefficients (*M3G*)

- A Galerkin approach can also be considered for the case that contains undamped deterministic eigenvalues and eigenvectors. For this case, the response vector is defined as follows

$$\begin{aligned}\tilde{\mathbf{u}}_{3G}(\omega,\theta) &\approx \sum_{j=1}^{n_r} c_j(\omega,\theta)\left(\frac{\phi_{0_j}^T\tilde{\mathbf{f}}_0}{\lambda_{0_j}-\omega^2+2\mathrm{i}\sqrt{\lambda_{0_j}}\omega\zeta}\right)\phi_{0_j} \\ &= \sum_{j=1}^{n_r} c_j\left(\omega,\theta\right)\gamma_{0_j}\left(\omega\right)\phi_{0_j}\end{aligned} \tag{85}$$

- Here $\gamma_{0_j}(\omega)$ and ϕ_{0_j} correspond to the deterministic scalars and the undamped deterministic eigenvector introduced in Equation (62).
- $c_j\left(\omega,\theta\right) \in \mathbb{C}$ are unknown constants which need to obtained for each realisation of each frequency.
- Similarly to the two preceding methods, the following set of equations is required to be solved for every realisation in each considered frequency

$$\mathbf{Z}_3(\omega,\theta)\mathbf{c}_3(\omega,\theta) = \mathbf{y}_3(\omega,\theta) \qquad j,k = 1,2,\ldots,n_r \tag{86}$$

Galerkin+projecting onto a deterministic basis with deterministic coefficients (*M3G*)

- where $\mathbf{Z}_{3_{kj}}(\omega,\theta) = \sum_{i=0}^{M}\left[\phi_{0_k}^T \mathbf{D}_i(\omega)\phi_{0_j}\right]\left[\xi_i(\theta)\gamma_{0_j}(\omega)\right]$;

$$\gamma_{0_j}(\omega) = \sum_{j=1}^{n_r}\left(\frac{\phi_{0_j}^T\tilde{\mathbf{f}}_0}{\lambda_{0_j}-\omega^2+2\mathrm{i}\sqrt{\lambda_{0_j}}\omega\zeta}\right)$$

$$\mathbf{y}_3(\omega) = \phi_{0_k}^T\tilde{\mathbf{f}}_0(\omega) \quad \forall \quad j,k = 1,2,\ldots n_r$$

and $\mathbf{c}_3(\omega,\theta)$ is the vector that contains the unknown constants $c_j(\omega,\theta)$

- The computational effort associated with this method is considerably lower than the other Galerkin methods as the scalars γ_{0_j} only need to be calculated once for each given frequency.
- The aim of this method is to incorporate the whole stochastic nature of system within the unknown scalars $c_j(\omega,\theta)$.
- This method is of significant interest as it is known that the behaviour of deterministic and stochastic systems can differ substantially especially if the coefficient of variation is significantly large.

Euler-Bernoulli cantilever beam

- An Euler-Bernoulli cantilever beam with stochastic bending modulus for a specified value of the correlation length and for different degrees of variability of the random field.

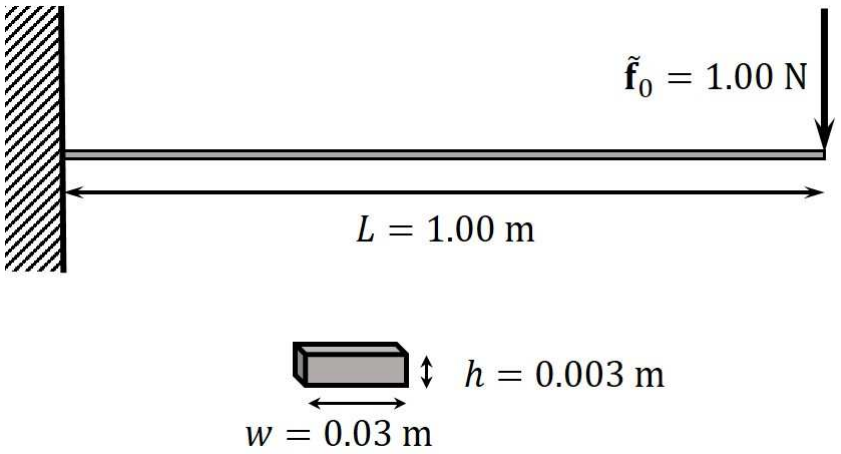

(a) Euler-Bernoulli beam

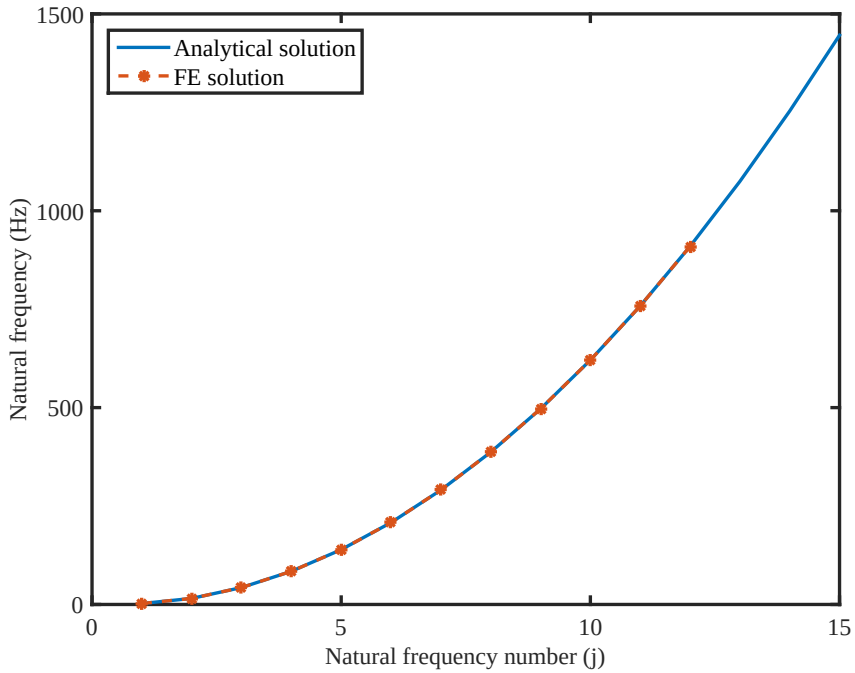

(b) Natural frequency distribution.

- Length : 1.0 m, $\overline{EI} = 4.66$ Nm^2.
- Load: Unit harmonic excitation at the free end of the beam.

Problem details

- The bending modulus of the cantilever beam is taken to be a homogeneous stationary Gaussian random field of the form

$$EI(x,\theta) = EI_0(1 + a(x,\theta)) \tag{87}$$

where x is the coordinate along the length of the beam, EI_0 is the estimate of the mean bending modulus, $a(x,\theta)$ is a zero mean stationary random field.

- The covariance kernel associated with this random field is

$$C_a(x_1,x_2) = \sigma_a^2 e^{-(|x_1-x_2|)/\mu_a} \tag{88}$$

where μ_a is the correlation length and σ_a is the standard deviation.

- A correlation length of $\mu_a = L/2$ is considered in the present numerical study.
- The K.L. expansion is truncated at a finite number of terms such that 90% variability is retained. The number of random variables $M = 4$.
- The amplitude of the vertical displacement at the tip of the beam under an unit harmonic point load at the free is considered.

Problem details

The random field is assumed to be Gaussian. The results are compared with the direct Monte Carlo Simulation results

- After applying the appropriate boundary conditions, the dimension of the corresponding discretized system is 200×200 ($N = 200$)
- direct MCS have been performed with 10,000 random samples and for two different values of standard deviation of the random field, $\sigma_a = 0.05, 0.2$.
- Constant modal damping is taken with 2% damping factor for all modes.
- The number of reduced mode used $n_r = 12$. This is a vast reduction as 188 terms have been discarded from each method.
- Galerkin error minimisation technique requires a linear set of 12×12 equations to solved for each sample. Although this could be seen as a tedious method, the dimension of the linear equations are much smaller than that of a 4th order polynomial chaos approach. Such an approach for the given configuration would require a $14,000 \times 14,000$ set of linear equations to be solved for each frequency step.

Mean of the response

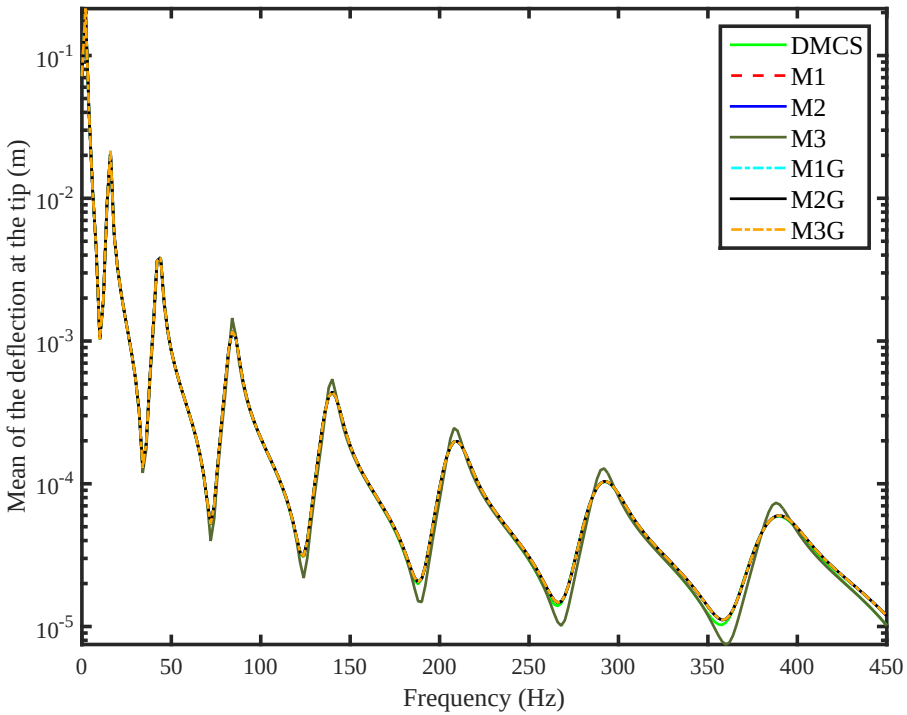

(a) $\sigma_a = 0.05$

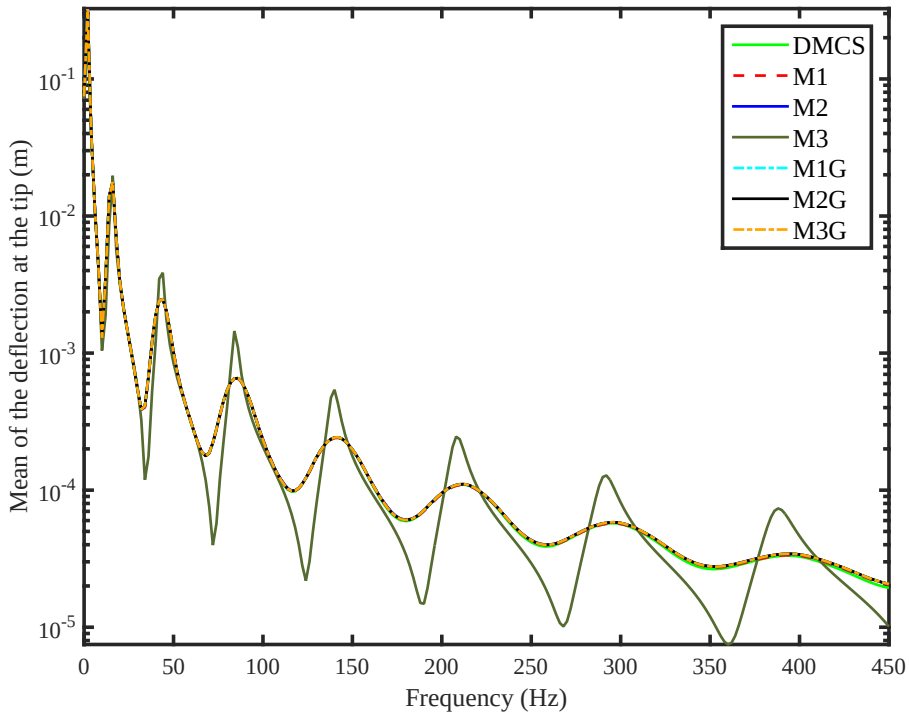

(b) $\sigma_a = 0.20$

The mean response is shown for two different values of the standard deviation of the bending rigidity: (a) $\sigma_a = 0.05$ (b) $\sigma_a = 0.20$.

Standard deviation of the response

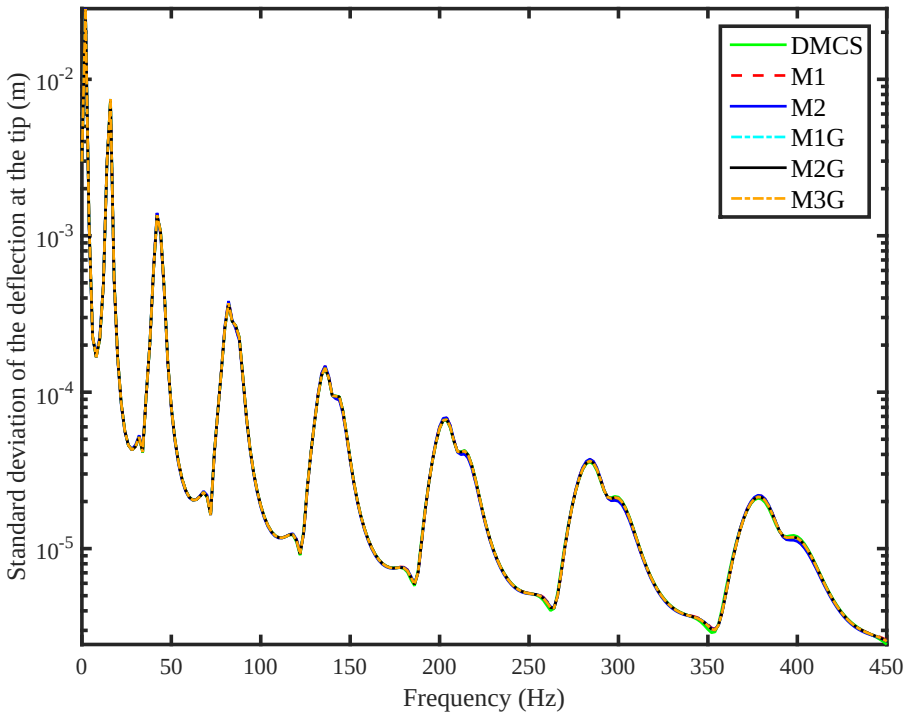

(a) $\sigma_a = 0.05$

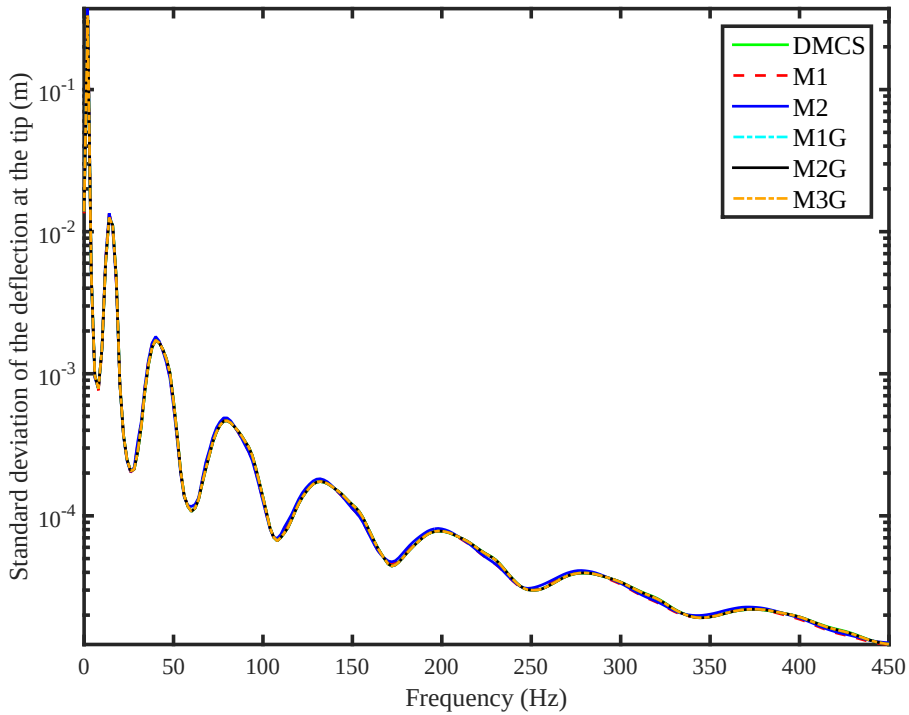

(b) $\sigma_a = 0.20$

The standard deviation response is shown for two different values of the standard deviation of the bending rigidity: (a) $\sigma_a = 0.05$ (b) $\sigma_a = 0.20$.

The probability density function of the response

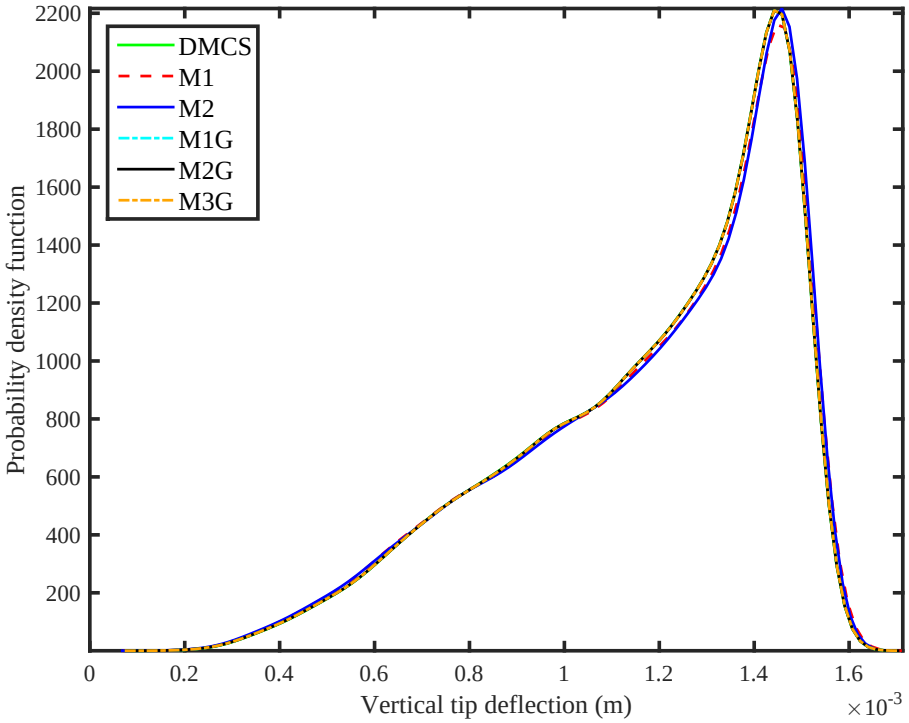

(a) $\sigma_a = 0.05$

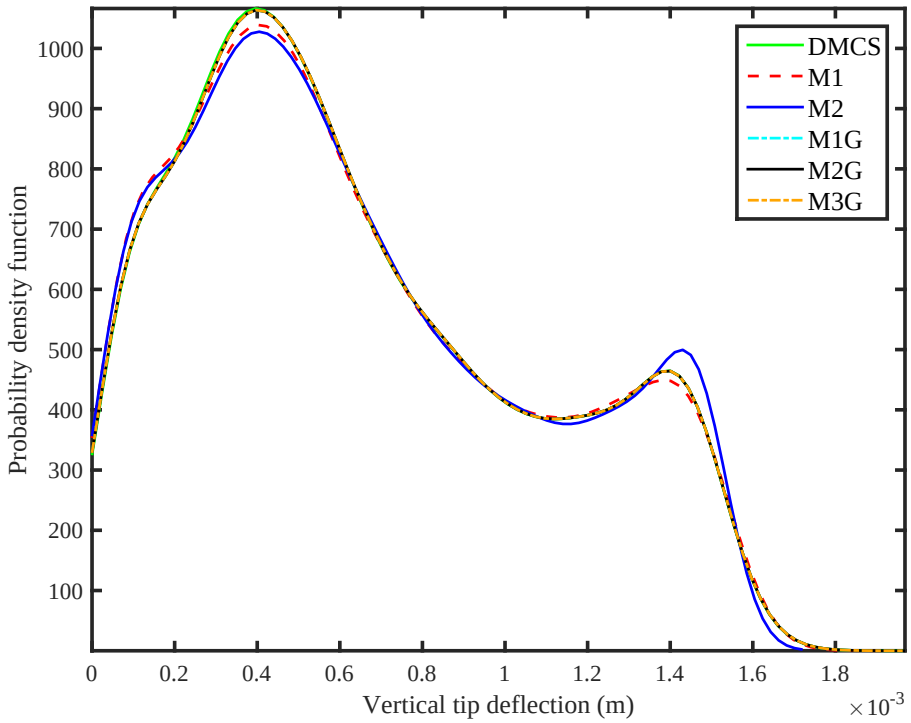

(b) $\sigma_a = 0.20$

The probability density function of the response at 84 Hz is shown for two different values of the standard deviation of the bending rigidity: (a) $\sigma_a = 0.05$ (b) $\sigma_a = 0.20$.

The error norm

- The L_2 relative error of the mean of the response vector for each frequency step is defined as follows

$$\hat{\varepsilon}^{\boldsymbol{\mu}}_{L_2}(\omega) = \frac{||\boldsymbol{\mu}_{DMCS}(\omega) - \boldsymbol{\mu}_{CM}(\omega)||_{L_2}}{||\boldsymbol{\mu}_{DMCS}(\omega)||_{L_2}} \tag{89}$$

- Here $\boldsymbol{\mu}_{DMCS}$ denotes the mean of the response vector obtained by using the *DMCS* method and $\boldsymbol{\mu}_{CM}$ denotes the mean of the response vector obtained by using a comparable method.
- This norm ensures that the error arising from each of the projection methods are characterised by a single value for each $\omega \in \Omega$.
- We obtain the log of the L_2 relative error for different values of n_r for both values of σ_a.

L_2 relative error for the mean response for $\sigma_a = 0.5$ for different n_r (y-axis) and different values of frequency (x-axis)

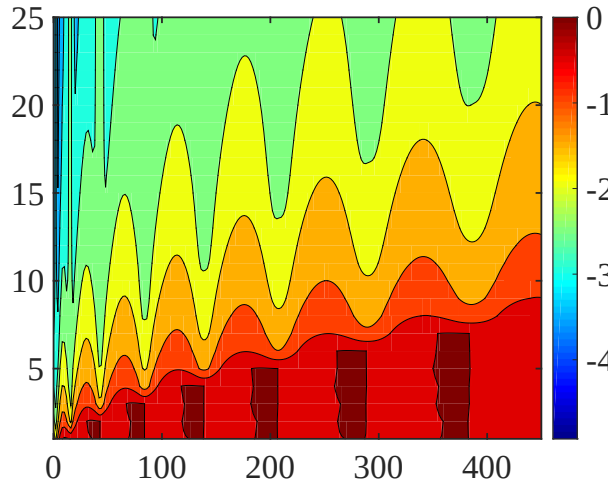

(a) M1

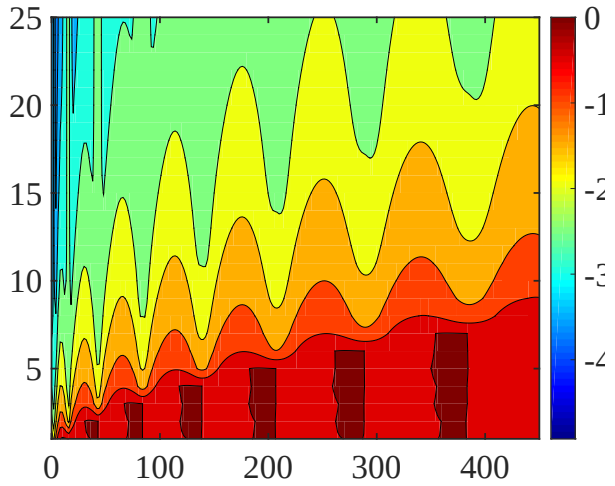

(b) M2

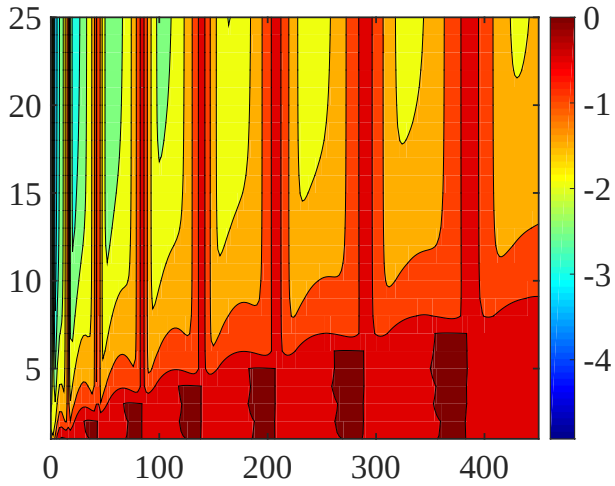

(c) M3

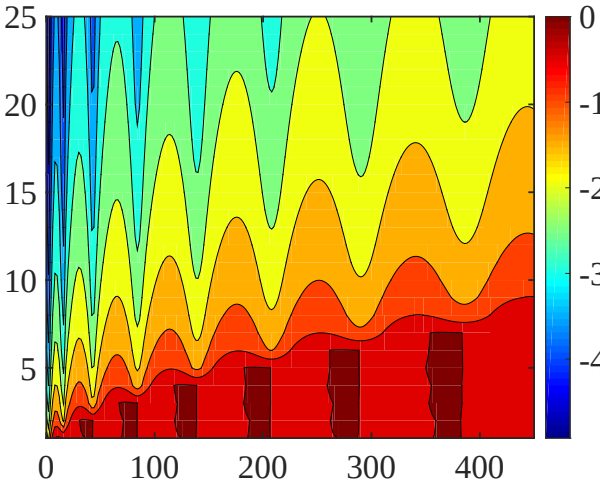

(d) M1G

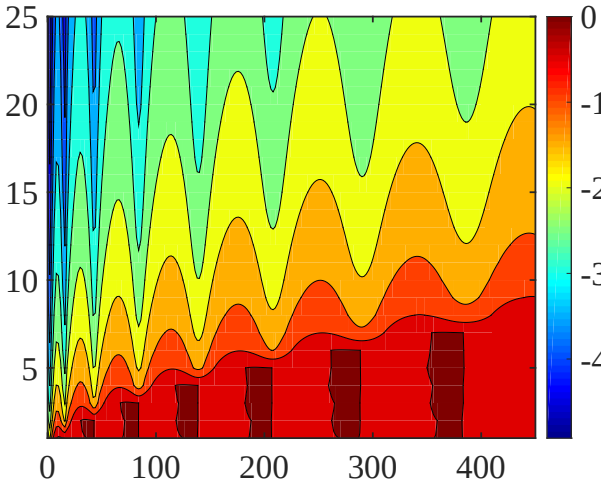

(e) M2G

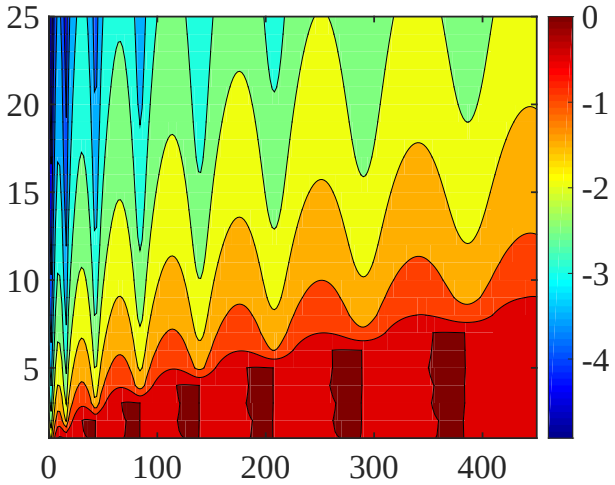

(f) M3G

L_2 relative error for the mean response for $\sigma_a = 0.20$ for different n_r (y-axis) and different values of frequency (x-axis)

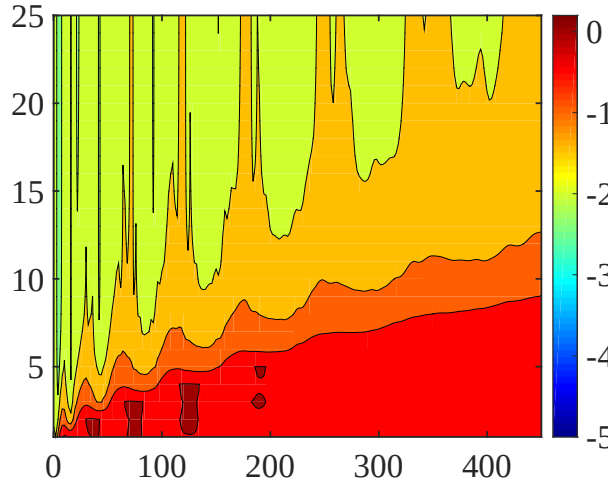

(a) M1

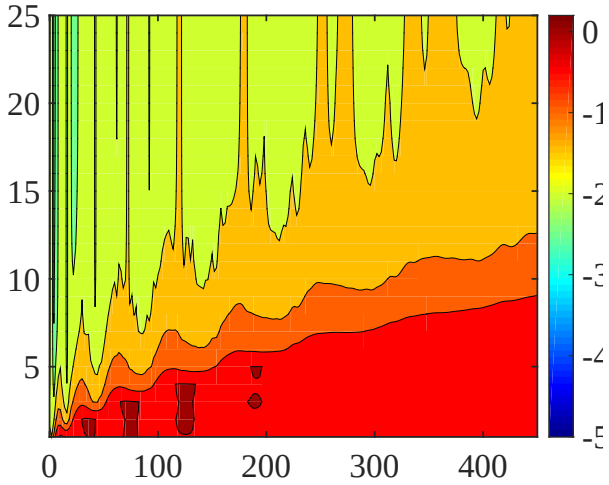

(b) M2

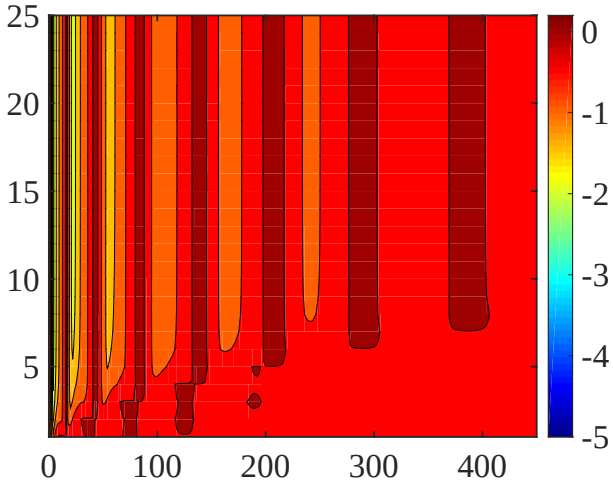

(c) M3

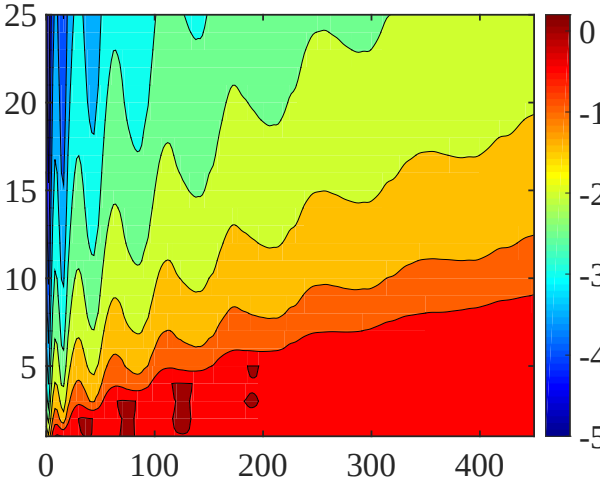

(d) M1G

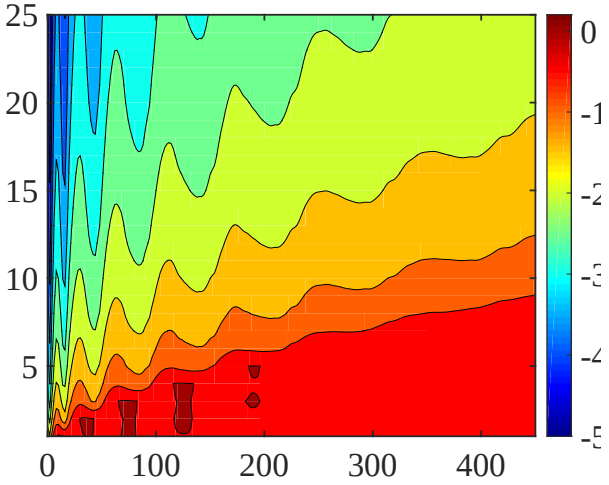

(e) M2G

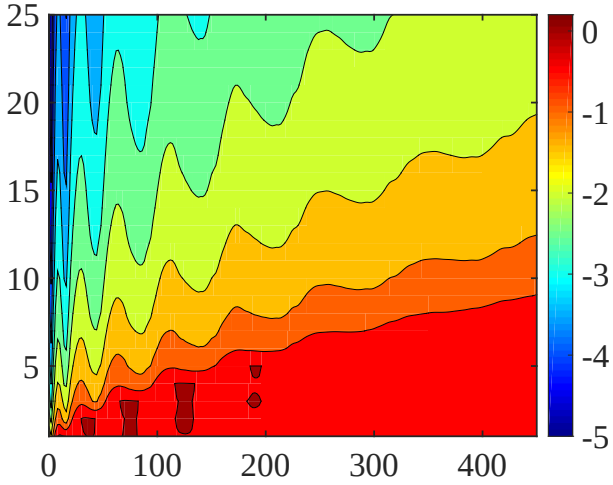

(f) M3G

L_2 relative error for the response standard deviation for $\sigma_a = 0.5$ for different n_r (y-axis) and different values of frequency (x-axis)

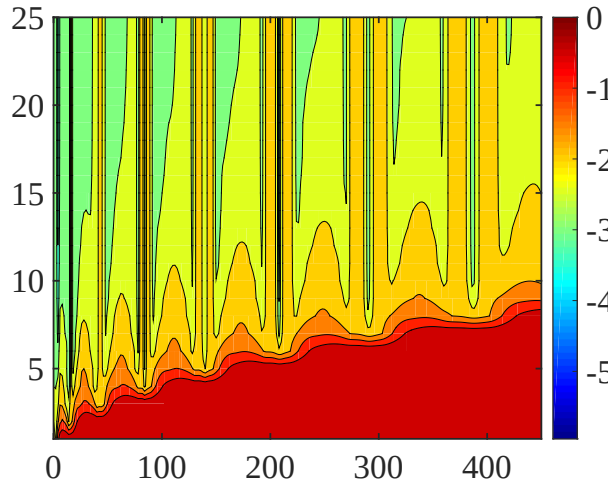

(a) M1

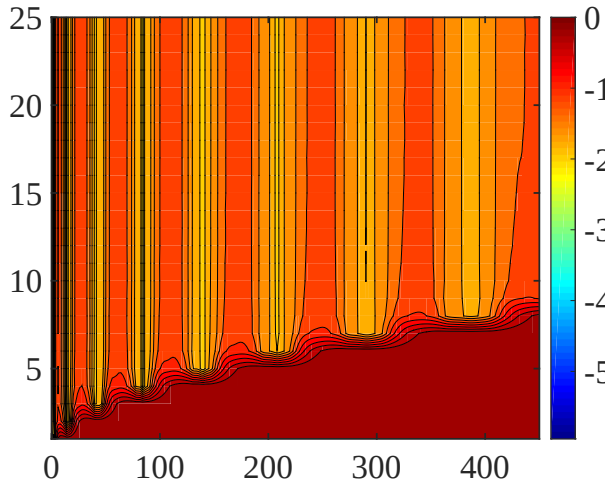

(b) M2

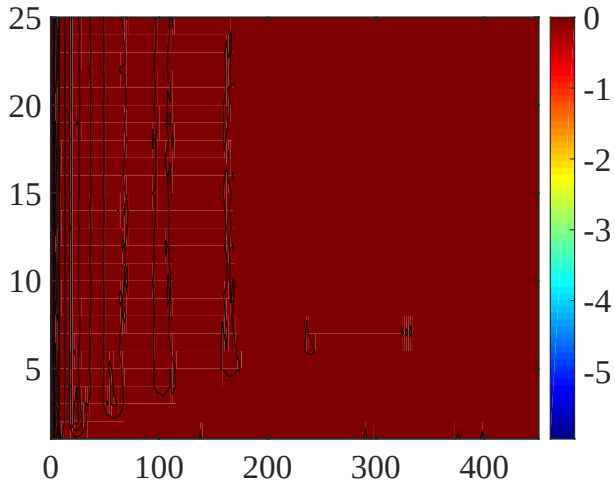

(c) M3

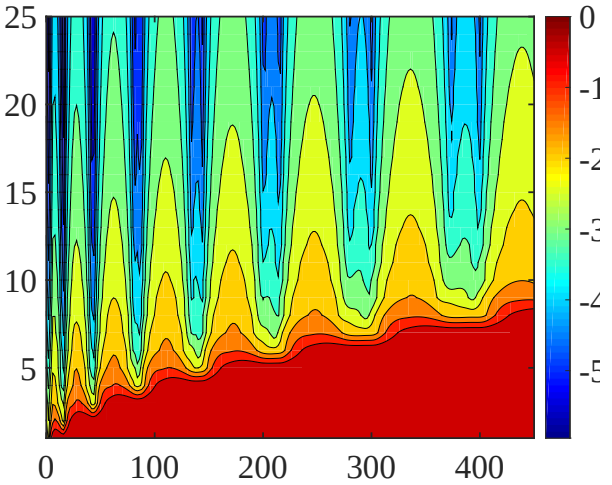

(d) M1G

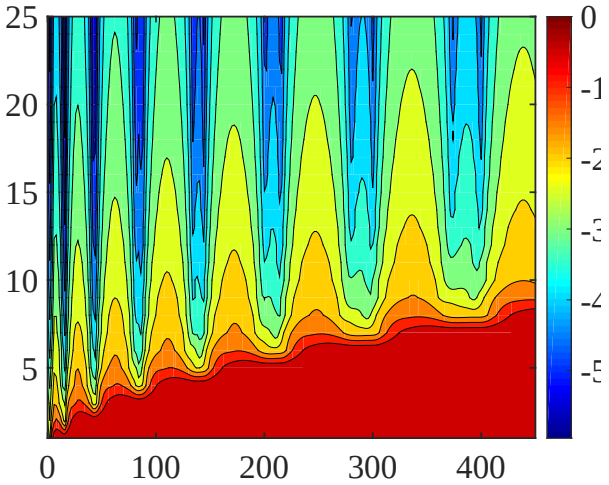

(e) M2G

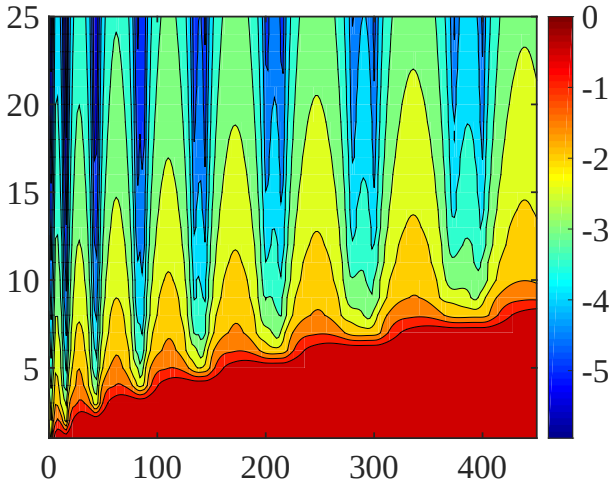

(f) M3G

L_2 relative error for the response standard deviation for $\sigma_a = 0.20$ for different n_r (y-axis) and different values of frequency (x-axis)

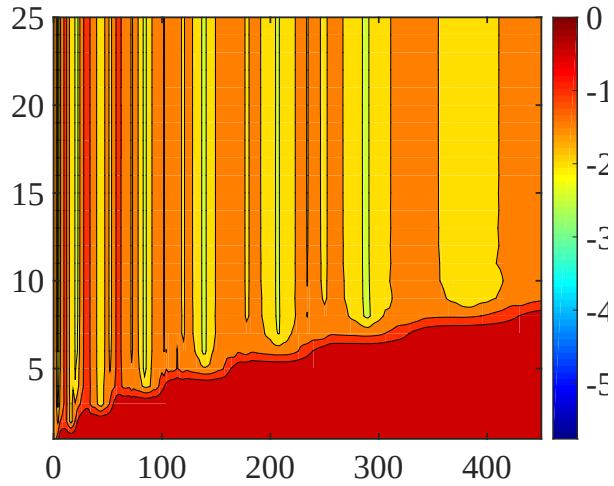

(a) M1

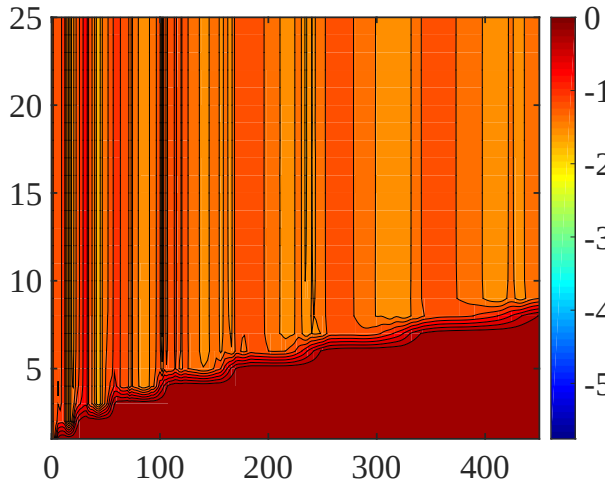

(b) M2

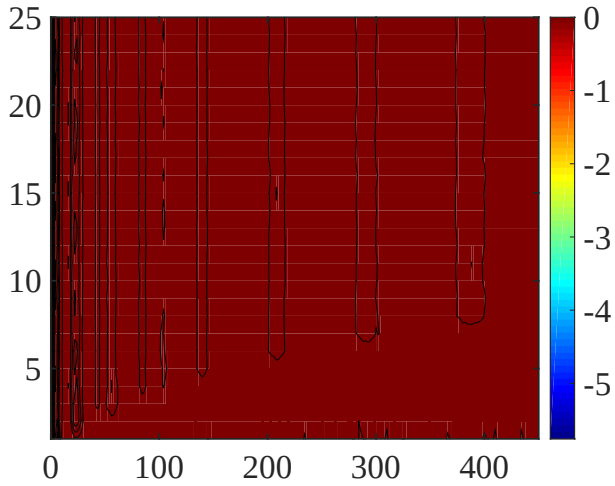

(c) M3

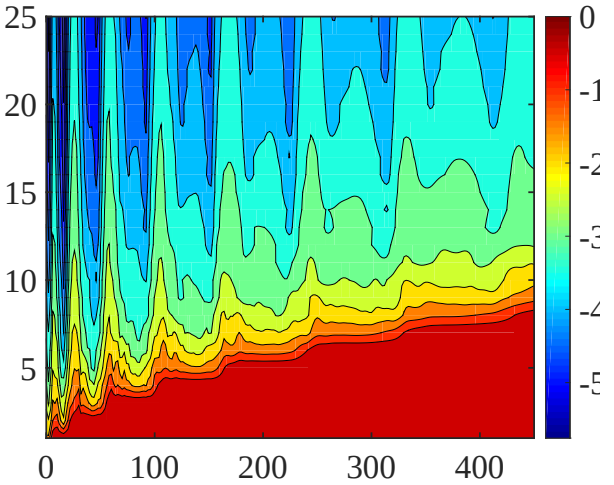

(d) M1G

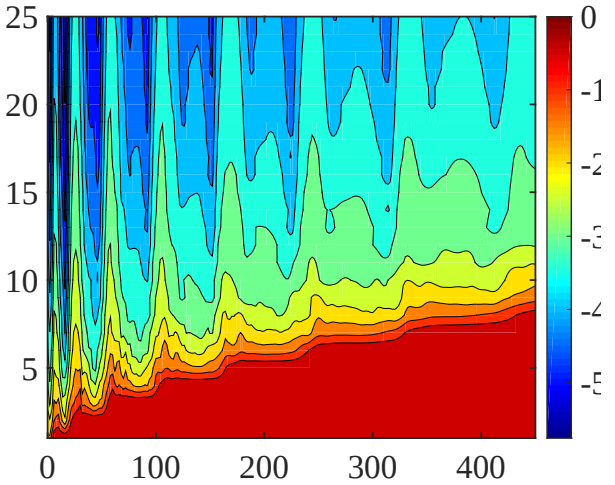

(e) M2G

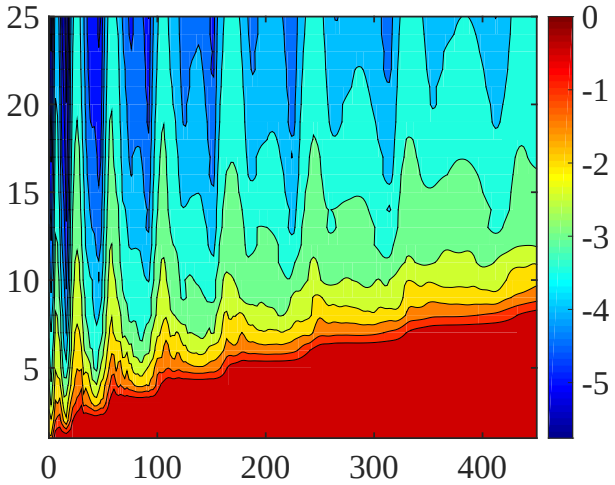

(f) M3G

L_2 relative error of the mean of the response

	Number of modes	M1	M2	M3	M1G	M2G	M3G
$\sigma_a = 0.05$	6	0.0071	0.0075	0.3126	0.0064	0.0064	0.0064
	9	0.0042	0.0048	0.3136	0.0024	0.0024	0.0024
	12	0.0038	0.0044	0.3139	0.0012	0.0012	0.0012
	15	0.0037	0.0044	0.3140	0.0007	0.0007	0.0007
	18	0.0037	0.0043	0.3141	0.0004	0.0004	0.0004
$\sigma_a = 0.20$	6	0.0193	0.0197	1.7920	0.0152	0.0152	0.0152
	9	0.0159	0.0154	1.7942	0.0054	0.0054	0.0054
	12	0.0158	0.0151	1.7942	0.0027	0.0027	0.0027
	15	0.0158	0.0151	1.7949	0.0016	0.0016	0.0016
	18	0.0158	0.0151	1.7952	0.0010	0.0100	0.0010

Table: The L_2 relative error of the mean of the response vector obtained by using the six reduced order methods for different values of n_r. The approximate L_2 relative error is shown for two different values of the standard deviation of the bending rigidity: (a) $\sigma_a = 0.05$ (b) $\sigma_a = 0.20$ at a frequency of 42 Hz.

Swansea University
Prifysgol Abertawe

L_2 relative error of the standard deviation of the response

	Number of modes	M1	M2	M3	M1G	M2G	M3G
$\sigma_a = 0.05$	6	0.0149	0.0166	1.0000	0.0004	0.0004	0.0004
	9	0.0147	0.0166	1.0000	0.0001	0.0001	0.0001
	12	0.0147	0.0166	1.0000	4×10^{-5}	4×10^{-5}	4×10^{-5}
	15	0.0147	0.0166	1.0000	1×10^{-5}	1×10^{-5}	1×10^{-5}
	18	0.0147	0.0166	1.0000	1×10^{-5}	1×10^{-5}	1×10^{-5}
$\sigma_a = 0.20$	6	0.0134	0.0214	1.0000	0.0005	0.0005	0.0005
	9	0.0132	0.0213	1.0000	0.0002	0.0002	0.0002
	12	0.0132	0.0213	1.0000	0.0001	0.0001	0.0001
	15	0.0132	0.0213	1.0000	0.0001	0.0001	0.0001
	18	0.0132	0.0213	1.0000	3×10^{-5}	3×10^{-5}	3×10^{-5}

Table: The approximate L_2 relative error of the standard deviation of the response vector obtained by using the six reduced order methods for different values of n_r. The approximate L_2 relative error is shown for two different values of the standard deviation of the bending rigidity: (a) $\sigma_a = 0.05$ (b) $\sigma_a = 0.20$ at a frequency of 42 Hz.

Kirchhoff-Love plate

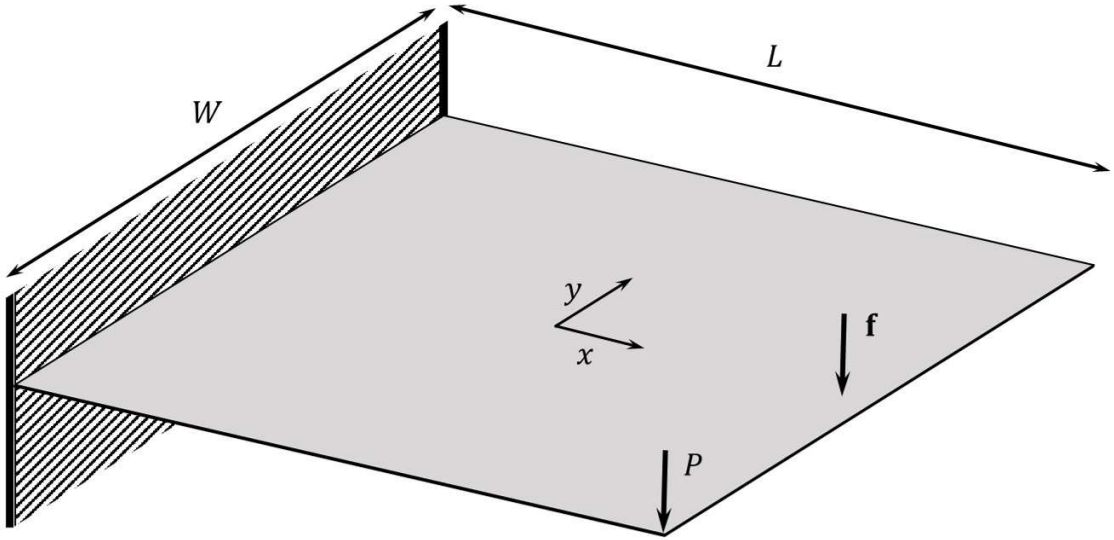

Figure: The configuration of the stochastic Kirchhoff-Love plate with a harmonic point load asserted at coordinate (0.42, 0.00).

- The rectangular plate under consideration has a length (L) of 1.00 m and a width (W) of 0.56 m.
- The centre of the plate has coordinates (0.00, 0.00).
- The plate is clamped along its width ($x = -0.50$ m), thus the displacement and rotational degrees of freedom along the clamped edge are zero.

Kirchhoff-Love plate

- The bending rigidity of the plate, D, can be assumed to be a stationary Gaussian random filed of the form

$$D(x, y, \theta) = \overline{D}(1 + a(x, y, \theta)) \tag{90}$$

- Here $a(x, y, \theta)$ is a stationary Gaussian field with zero mean and x and y the coordinate directions of the length and width of the plate. $\overline{D}$ corresponds to the deterministic value of the bending rigidity of the plate.
- The correlation function of the random field can be assumed to take the following form

$$C_a(x_1, x_2, y_1, y_2) = \sigma_a^2 e^{-(|x_1 - x_2|)/\mu_x} e^{-(|y_1 - y_2|)/\mu_y} \tag{91}$$

  where σ_a is the standard deviation of the bending rigidity, and μ_x and μ_y are the correlation lengths for both the x and y directions respectively.
- The forcing vector is again deemed deterministic with an unit norm. This is applied as a harmonic point load at coordinate $(0.42, 0.00)$. The deterministic modal damping matrix consists of a 2% damping factor for each mode.

Kirchhoff-Love plate

- The parameters of the plate are as follows: thickness $h = 0.003$ m, mass density $\rho = 7860$ kg m^{-3} and a Young's modulus of $E = 200 \times 10^9$ Nm^{-2} thus resulting in $D_0 = 494.51$ Nm.
- The correlation length is set at $\mu_x = \frac{L}{5}$ i.e. a fifth of respective length in the x direction, and set at $\mu_y = \frac{W}{5}$ in the y direction.
- The thin plate has been divided into 25 elements in the x direction and 14 elements in the y direction. This leads to the system containing 1,125 degrees of freedom ($N = 1125$).
- Three terms have been retained in the KL expansion along both the x and y axis. Thus by using a tensor product the full KL expression for the whole system contains 9 random variables ($M = 9$).
- The response of the plate has been analysed for two different values of the standard deviation

$$\sigma_a = \{0.05, 0.15\} \tag{92}$$

Kirchhoff-Love plate

- For the case of the unit amplitude harmonic point load acting on plate, the frequency range under consideration is $0 - 200$ Hz at an interval of 2 Hz.
- This corresponds to considering 101 different frequency values. 5,000 samples have been considered for each frequency step. 5,000 samples gives a satisfactory convergence for the first two moments of the quantities of interest.
- For each of the proposed methods thirty terms have been retained in their respective summations, hence $n_r = 30$.
- If all the terms were retained, all the summations would contain 1,125 terms.
- The methods implementing the Galerkin error minimisation technique require a linear set of 30×30 equations to be solved for each sample.
- In comparison, a fourth order polynomial chaos method would require a $804,375 \times 804,375$ set of linear equations to be solved for each frequency step. Solving a set of linear equations of such a high dimension would require a large computational effort.

Mean of the response at the corner of the plate $(0.50, -0.28)$

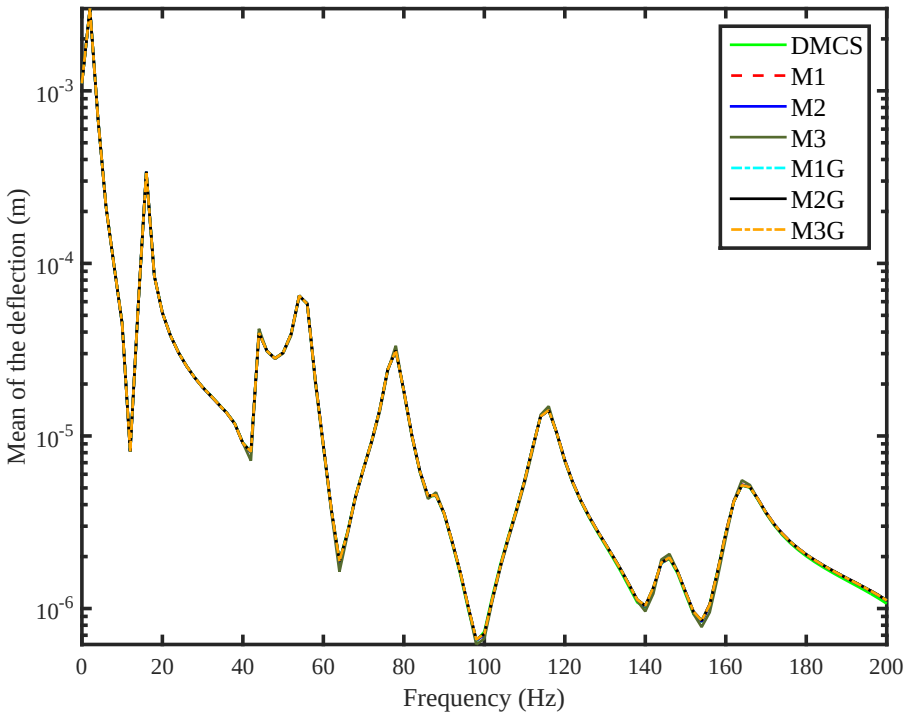

(a) $\sigma_a = 0.05$

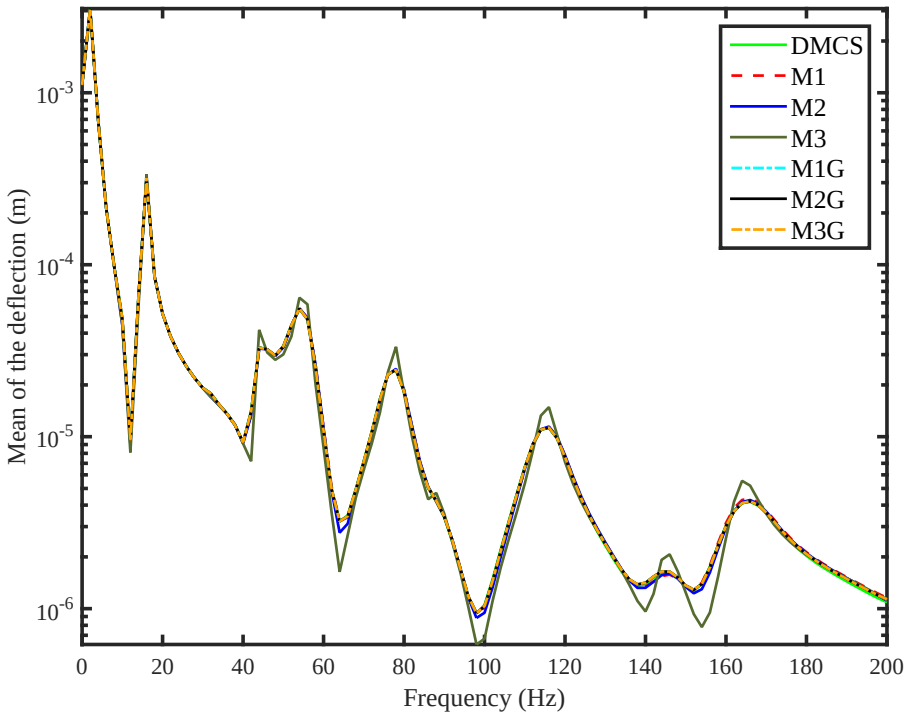

(b) $\sigma_a = 0.15$

The mean response is shown for two different values of the standard deviation of the bending rigidity: (a) $\sigma_a = 0.05$ (b) $\sigma_a = 0.15$.

Standard deviation of the response at the corner of the plate $(0.50, -0.28)$

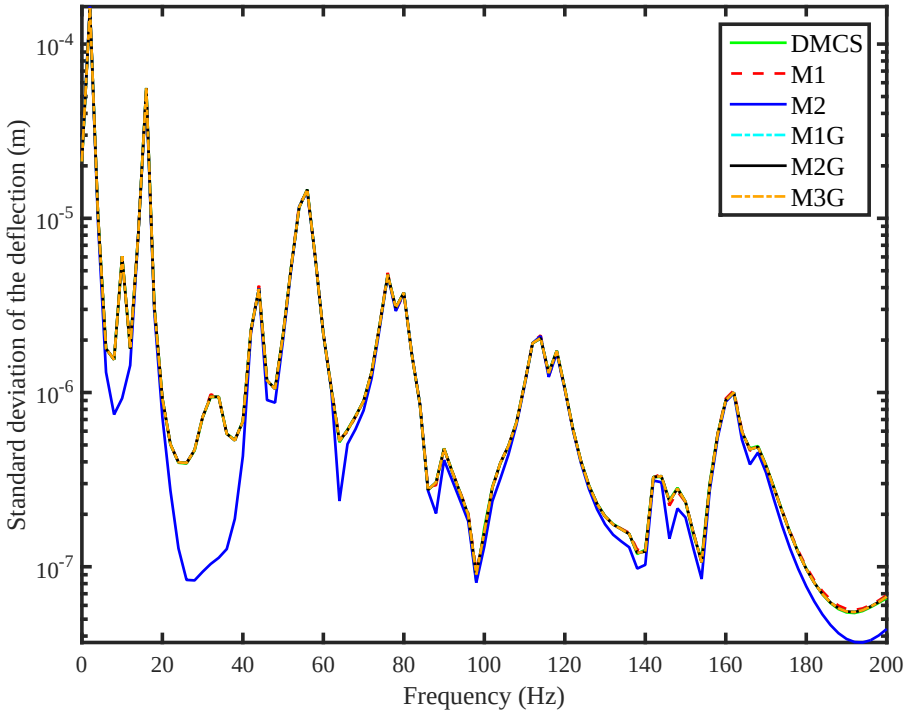

(a) $\sigma_a = 0.05$

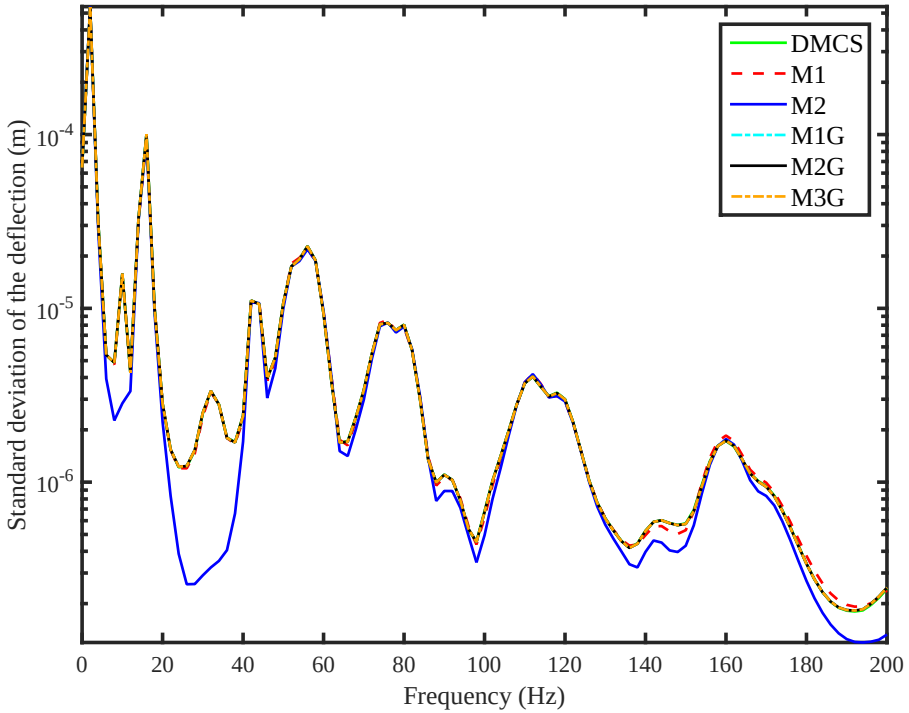

(b) $\sigma_a = 0.15$

The standard deviation response is shown for two different values of the standard deviation of the bending rigidity: (a) $\sigma_a = 0.05$ (b) $\sigma_a = 0.15$.

The L_2 relative error of the mean of the response

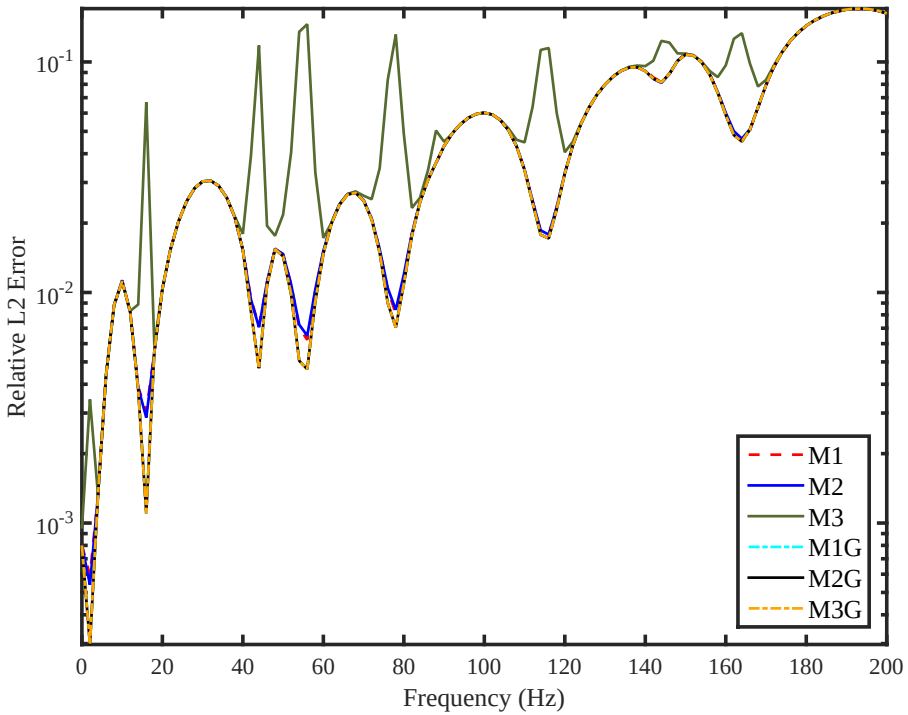

(a) $\sigma_a = 0.05$

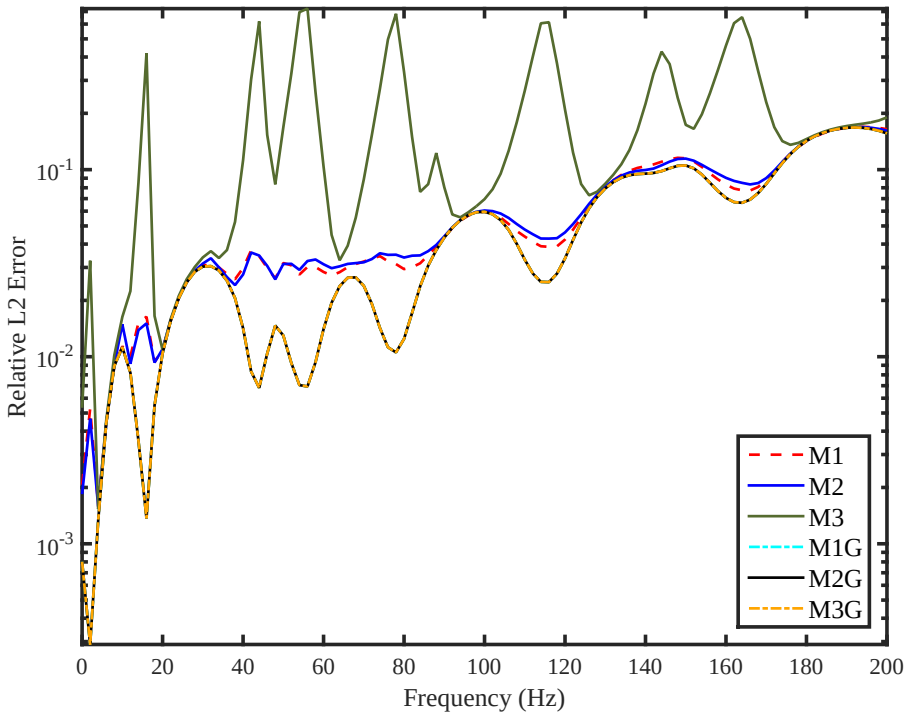

(b) $\sigma_a = 0.15$

The relative error norm of the mean is shown for two different values of the standard deviation of the bending rigidity: (a) $\sigma_a = 0.05$ (b) $\sigma_a = 0.15$.

The L_2 relative error of the response standard deviation

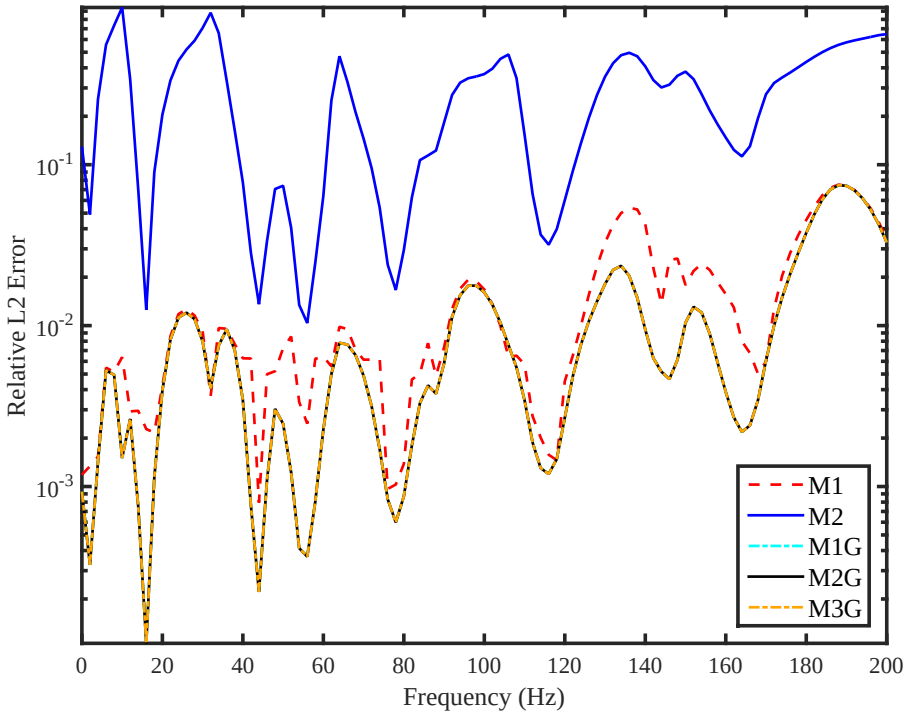

(a) $\sigma_a = 0.05$

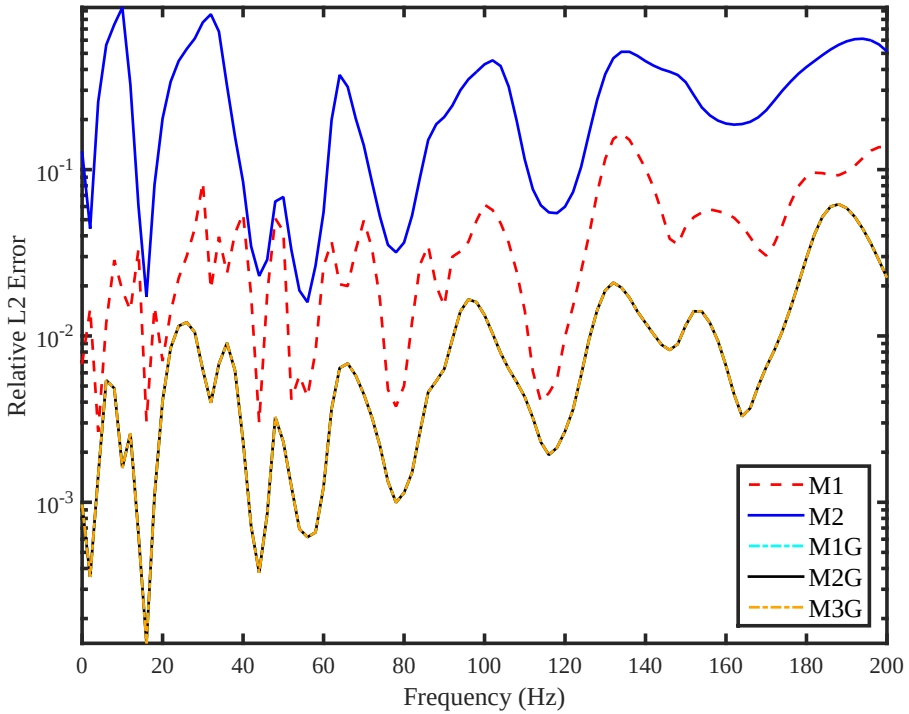

(b) $\sigma_a = 0.15$

The relative error norm of the standard deviation is shown for two different values of the standard deviation of the bending rigidity: (a) $\sigma_a = 0.05$ (b) $\sigma_a = 0.15$.

The probability density function of the response at 168 Hz at $(0.42, 0.00)$

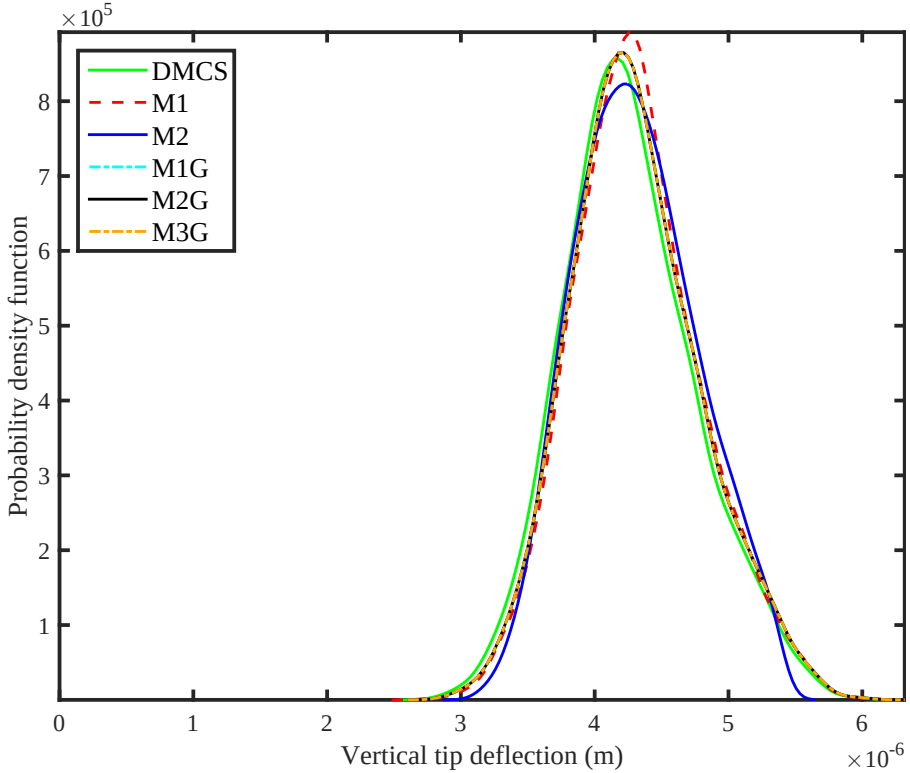

(a) $\sigma_a = 0.05$

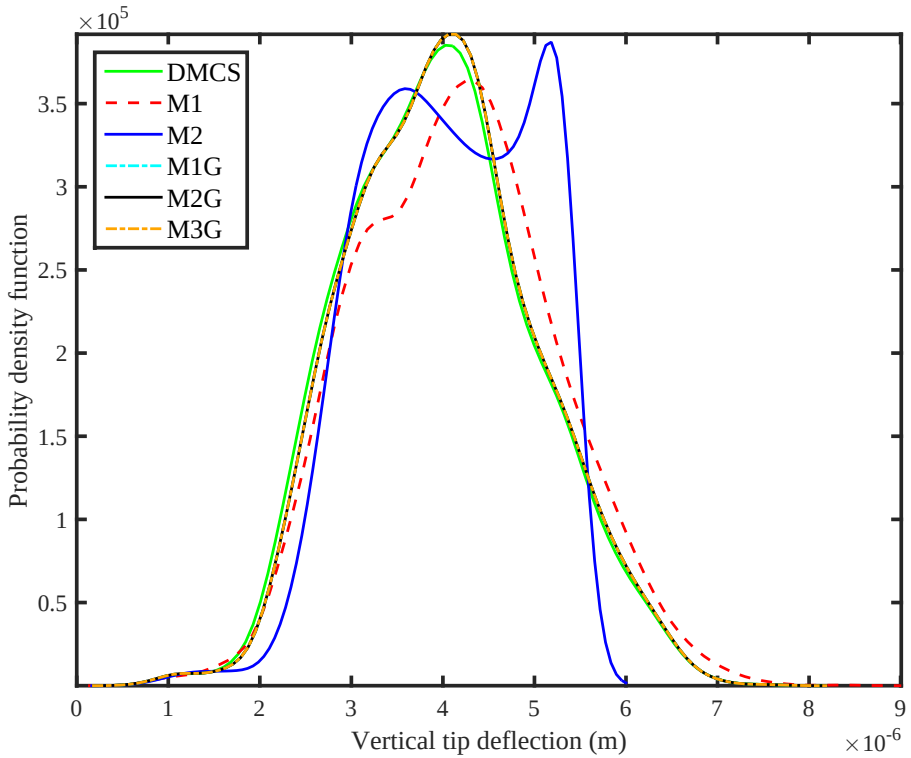

(b) $\sigma_a = 0.15$

168 Hz corresponds to the 16th deterministic resonance frequency. The probability density function of the response at $(0.42, 0.00)$ is shown for two different values of the standard deviation of the bending rigidity: (a) $\sigma_a = 0.05$ (b) $\sigma_a = 0.15$.

Summary and Conclusion

- Three projection methods have been developed by utilising the random eigenvalue problem.
- The first method utilises both random eigenvalues and eigenvectors, the second random eigenvalues and deterministic eigenvectors and the third only uses deterministic eigensolutions.
- In order to reduce the computational effort associated with each of these methods, the random eigensolutions have been approximated by a first order perturbation and only the dominant projection terms have been retained.
- Due to the approximations and the reduced modal basis, three additional projection methods have been proposed. These methods utilise a sample based Galerkin error minimization approach in order to lower the error.
- Both the coefficients and their corresponding basis have been computed by utilising the stochastic and deterministic eigensolutions of the structural system.
- The computational effort is reduced by approximating the stochastic eigensolutions and by reducing the modal basis.
- To compensate for the error induced by the computational reduction a sample based Galerkin error minimization approach is presented.

Swansea University
Prifysgol Abertawe

Summary and Conclusion

- If the sample based Galerkin error minimization approach is omitted it is necessary for both the coefficients and their associated basis to be stochastic in order to capture an accurate response for a system.
- If the Galerkin error minimization approach is applied calculating the stochastic eigensolutions is unwarranted. The accuracy of the response is equally as good if deterministic basis and deterministic coefficients are utilised.
- It is apparent that if the sample based Galerkin error minimization approach were not to be implemented the stochastic properties of the random eigenvalues and eigenvectors must be retained in order to capture the variation of the governing equation.
- A surprising outcome is that the application of the Galerkin error minimization approach in conjunction with projecting onto a deterministic basis with deterministic coefficients (*M*3*G*) produces a level of accuracy compared with to any of the other proposed methods. Although appears to be non-intuitive, our study leads us to suggest that this simple approach has significant potential for analysing stochastic structural systems.

Swansea University
Prifysgol Abertawe

Summary and Conclusion

Method	Form of the response vector	Coefficient	Basis	Vector of Galerkin coefficients
$M1$	$\sum_{j=1}^{n_r} \alpha_j(\omega,\theta)\mathbf{a}_j(\theta)$	$\frac{\boldsymbol{\phi}_j^T(\theta)\tilde{\mathbf{f}}_0}{\lambda_j(\theta)-\omega^2+2\mathrm{i}\sqrt{\lambda_j(\theta)}\omega\zeta}$	$\boldsymbol{\phi}_j(\theta)$	-
$M2$	$\sum_{j=1}^{n_r} \beta_j(\omega,\theta)\mathbf{b}_j$	$\frac{\boldsymbol{\phi}_{j_0}^T\tilde{\mathbf{f}}_0}{\lambda_j(\theta)-\omega^2+2\mathrm{i}\sqrt{\lambda_j(\theta)}\omega\zeta}$	$\boldsymbol{\phi}_{j_0}$	-
$M3$	$\sum_{j=1}^{N} \gamma_j(\omega)\mathbf{c}_j$	$\frac{\boldsymbol{\phi}_{j_0}^T\tilde{\mathbf{f}}_0}{\lambda_{j_0}-\omega^2+2\mathrm{i}\sqrt{\lambda_{j_0}}\omega\zeta}$	$\boldsymbol{\phi}_{j_0}$	-
$M1G$	$\sum_{j=1}^{n_r} c_j(\omega,\theta)\alpha_j(\omega,\theta)\mathbf{a}_j(\theta)$	$\frac{\boldsymbol{\phi}_j^T(\theta)\tilde{\mathbf{f}}_0}{\lambda_j(\theta)-\omega^2+2\mathrm{i}\sqrt{\lambda_j(\theta)}\omega\zeta}$	$\boldsymbol{\phi}_j(\theta)$	$\mathbf{Z}_1^{-1}(\theta,\omega)\mathbf{y}_1(\theta,\omega)$
$M2G$	$\sum_{j=1}^{n_r} c_j(\omega,\theta)\beta_j(\omega,\theta)\mathbf{b}_j$	$\frac{\boldsymbol{\phi}_{j_0}^T\tilde{\mathbf{f}}_0}{\lambda_j(\theta)-\omega^2+2\mathrm{i}\sqrt{\lambda_j(\theta)}\omega\zeta}$	$\boldsymbol{\phi}_{j_0}$	$\mathbf{Z}_2^{-1}(\theta,\omega)\mathbf{y}_2(\omega)$
$M3G$	$\sum_{j=1}^{n_r} c_j(\omega,\theta)\gamma_j(\omega)\mathbf{c}_j$	$\frac{\boldsymbol{\phi}_{j_0}^T\tilde{\mathbf{f}}_0}{\lambda_{j_0}-\omega^2+2\mathrm{i}\sqrt{\lambda_{j_0}}\omega\zeta}$	$\boldsymbol{\phi}_{j_0}$	$\mathbf{Z}_3^{-1}(\theta,\omega)\mathbf{y}_3(\omega)$

Table: Summary of the proposed methods

Future work - EPSRC Program Grant

EPSRC Pioneering research and skills

Engineering and Physical Sciences Research Council

GoW Search Go

Home | GoW Home | Back | Research Areas | Topic | Sector | Scheme | Region | Theme | Organisation | Partners

Details of Grant

EPSRC Reference:	**EP/R006768/1**		
Title:	**Digital twins for improved dynamic design**		
Principal Investigator:	**Wagg, Professor DJ**		
Other Investigators:	**Au, Professor S**	**Elliott, Professor S**	**Clarkson, Professor J**
	Langley, Professor RS	**Neild, Professor SA**	**Friswell, Professor MI**
	Worden, Professor K		
Researcher Co-Investigators:			
Project Partners:	**Airbus Group Limited**	**EDF Energy**	**Leonardo (UK)**
	LOC Group (London Offshore Consultants)	**Romax Technology Limited**	**Schlumberger**
	Siemens	**Stirling Dynamics Ltd**	**Ultra Electronics Ltd**
Department:	**Mechanical Engineering**		
Organisation:	**University of Sheffield**		
Scheme:	**Programme Grants**		
Starts:	**01 February 2018**	Ends: **31 January 2023**	Value (£): **5,112,624**
EPSRC Research Topic Classifications:	**Design Engineering**	**Statistics & Appl. Probability**	
EPSRC Industrial Sector Classifications:	**Aerospace, Defence and Marine**	**Energy**	
Related Grants:			

Panel History:

Panel Date	Panel Name	Outcome
01 Nov 2017	**Programme Grant Interviews - 1 November 2017 (Engineering)**	**Announced**

Summary on Grant Application Form

The aim of this proposal is to create a robustly-validated virtual prediction tool called a "digital twin". This is urgently needed to overcome limitations in current industrial practice that increasingly rely on large computer-based models to make critical design and operational decisions for systems such as wind farms, nuclear power stations and aircraft. The digital twin is much more than just a numerical model: It is a "virtualised" proxy version of the physical system built from a fusion of data with models of differing fidelity, using novel techniques in uncertainty analysis, model reduction, and experimental validation. In this project, we will deliver the transformative new science required to generate digital twin technology for key sectors of UK industry: specifically power generation, automotive and aerospace. The results from the project will empower industry with the ability to create digital twins as predictive tools for real-world problems that (i) radically improve design methodology leading to significant cost savings, and (ii) transform uncertainty management of key industrial assets, enabling a step change reduction in the associated operation and management costs. Ultimately, we envisage that the scientific advancements proposed here will revolutionise the engineering design-to-decommission cycle for a wide range of engineering applications of value to the UK.

Some of our recent papers on this topic

1. Pryse, S. E., Adhikari, S., and Kundu, A., Projection methods for stochastic dynamic systems: A frequency domain approach, Computer Methods in Applied Mechanics and Engineering, Vol 338, 2018, pp. 412-439.
2. Pryse, S. E., Adhikari, S., and Kundu, A., Sample-based and sample-aggregated Galerkin projection schemes for structural dynamics, Probabilistic Engineering Mechanics, Vol 54, 2018, pp. 118-130.
3. Pryse, S. E. and Adhikari, S., "Stochastic finite element response analysis using random eigenfunction expansion", Computers and Structures, 192[11] (2017), pp. 1-15.
4. Jacquelin, E., Dessombz, O., Sinou, J.-J., Adhikari, S., and Friswel, M. I., Polynomial chaos based eXtended Pade expansion in structural dynamics, International Journal for Numerical Methods in Engineering, Vol. 111, No. 12, 2017, pp. 1170-1191.
5. Jacquelin, E., Adhikari, S., Sinou, J.-J., and Friswell, M. I., The role of roots of orthogonal polynomials in the dynamic response of stochastic systems, ASCE Journal of Engineering Mechanics, Vol. 142, No. 8, 2015, pp. 06016004:1-8.
6. Jacquelin, E., Friswel, M. I., Adhikari, S., Dessombz, O., and Sinou, J.-J., Polynomial chaos expansion with random and fuzzy variables, Mechanical Systems and Signal Processing, Vol. 75, No. 6, 2016, pp. 41-56.
7. Kundu, A., Adhikari, S., and Friswell, M. I., Transient response analysis of randomly parametrized finite element systems based on approximate balanced reduction, Computer Methods in Applied Mechanics and Engineering, Vol. 285, No. 3, 2015, pp. 542-570.
8. Jacquelin, E., Adhikari, S., Sinou, J.-J., and Friswell, M. I., Polynomial chaos expansion and steady-state response of a class of random dynamical systems, ASCE Journal of Engineering Mechanics, Vol. 106, No. 6, 2015, pp. 061901:1-4.
9. Kundu, A. and Adhikari, S., Dynamic analysis of stochastic structural systems using frequency adaptive spectral functions, Probabilistic Engineering Mechanics, Vol. 39, No. 1, 2015, pp. 23-38.
10. Kundu, A. and Adhikari, S., Transient response of structural dynamic systems with parametric uncertainty, ASCE Journal of Engineering Mechanics, Vol. 140, No. 2, 2014, pp. 315-331.

Swansea University
Prifysgol Abertawe